8 FAILURE AND INITIAL YIELD CRITERIA

In the previous chapters, we discussed constitutive relations with an increasing degree of complexity. We started out with linear and nonlinear elasticity where a one-to-one relation exists between the current stresses and current strains. We then moved to materials where the constitutive relation is given in an incremental fashion, i.e. the current stress or strain state can only be obtained by an integration of the load history. This means that the response becomes history dependent.

For a time-independent material response, the most important class of incremental constitutive relations that are able to distinguish between loading and unloading in a realistic manner is provided by the *plasticity theory*; in the following chapters, we will discuss various aspects of this theory.

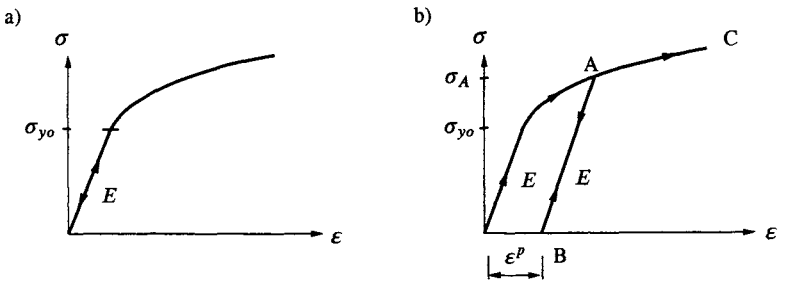

Figure 8.1: a) Loading below the initial yield stress σ_{yo}; b) loading above the initial yield stress.

As a beginning to the plasticity theory, in this chapter we will deal with criteria which tell us whether plastic deformations - i.e. yielding of the material - or failure occurs. For this purpose consider the uniaxial stress-strain curve shown in Fig. 8.1. If the stress is below the *initial yield stress* σ_{yo}, the material is assumed to behave linear elastic with a stiffness given by Young's modulus E, cf. Fig. 8.1a). If the material is loaded to the stress σ_A, cf. Fig. 8.1b),

yielding occurs and at unloading to point B we are left with the *plastic strain* ε^p. The unloading from A to B is assumed to occur elastically with the stiffness E. Reloading from point B first follows the linear path BA and at point A yielding is again activated and the path AC is then traced as if the unloading at point A had never occurred. It appears that for unloading from point A and subsequent reloading, the stress σ_A that is needed to activate further plastic deformations has increased when compared with the initial yield stress σ_{yo}. We therefore have a *hardening* effect.

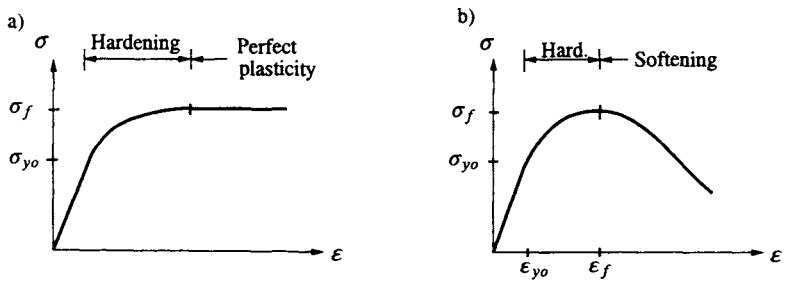

Figure 8.2: a) Hardening and perfect plasticity; b) hardening and softening plasticity.

If the strain is increased sufficiently, we may reach the situations illustrated in Fig. 8.2. After a hardening phase, we reach in Fig. 8.2a) a maximum stress σ_f - the *failure stress* - and with continued straining, the stress remains at the value σ_f; that is we have now reached a situation of *perfect* or *ideal plasticity*. In Fig. 8.2b), on the other hand, after having obtained the failure stress σ_f, the stress decreases with continued deformation. This so-called *softening* behavior is typical for materials like concrete, soil and rocks and other cementitious materials when loaded in compression.

In this chapter, we will be concerned with the identification of the initial yield stress σ_{yo} and the failure stress σ_f. Later on, in the plasticity theory, we will establish rules for how the material behaves when loaded beyond the initial yield stress.

It is obvious that the initial yield stress and the failure stress are important engineering quantities. Whereas their identification is trivial for uniaxial stress states, this is not the case for general stress states. In general, the stress state is defined by the stress tensor which comprises six independent stress components; the task is therefore to determine critical combinations of these components that result in initial yielding or failure of the material. We will see that for isotropic materials, it is possible to obtain a large amount of information on the general form of such criteria without knowing the specific material.

It is worthwhile to scrutinize the term 'failure stress' a little further. As apparent from Fig. 8.2, this term is slightly misleading since the material does not necessarily lose its load-carrying capacity when the 'failure' stress σ_f is

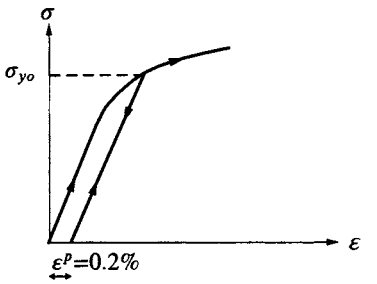

Figure 8.3: Definition of σ_{yo} based on 0.2% off-set strain

reached. Rather, the stress σ_f refers to that peak stress a homogeneously loaded specimen can carry and therefore the term *ultimate stress* seems more appropriate. However, by tradition we will use the word failure stress.

While the identification of the failure stress is unambiguous, this is not the case for the initial yield stress σ_{yo}. The reason is that most materials exhibit a smooth transition from the elastic region to the elastic-plastic region with no distinct point where yielding is initiated; examples are shown in Fig. 8.2. The identification of the initial yield stress σ_{yo} therefore becomes a matter of convention. In handbooks, the initial yield stress σ_{yo} for metals and steel is most often identified as the so-called $\sigma_{0.2}$-*stress*, i.e. the stress at which the remaining plastic strain after unloading equals 0.2%. This definition is illustrated in Fig. 8.3 and the remaining plastic strain is often called the *off-set strain*. Since a plastic strain of 0.2% is not insignificant, this definition of σ_{yo} is rather crude and in most scientific experimental investigations a much smaller off-set strain is used.

For general stress states, the conditions for failure or initial yielding are called *failure* or *initial yield criteria* respectively. Since they can be treated in a unified manner, we will often simply use the word criterion. We will see that stress invariants play an extremely important role in failure and yield criteria and we will therefore make extensive use of the results obtained in Chapter 3.

In general, the material is anisotropic, i.e. for a given loading the orientation of the material influences its response. We seek a criterion, i.e. a function, which takes the value of zero when the conditions for initial yielding or failure are fulfilled.

Consider a specimen of a homogeneous material loaded by a homogeneous stress state. Considering proportional loading, we will assume that the yield or failure criterion is independent of the loading rate. Under these conditions, the initial yield or failure criterion can only depend on the stress tensor σ_{ij}, i.e.

$$\boxed{F(\sigma_{ij}) = 0} \tag{8.1}$$

When this condition is fulfilled, initial yielding and failure occur in the material. We know from Sections 6.5 and 6.6 that if anisotropic materials are considered,

say orthotropy, then the yield or failure criterion, in addition to the stresses σ_{ij}, also depends on some structural tensors. However, at the present stage it is not of importance to include such structural tensors among the variables entering the yield or failure criterion.

By convention the function F is normalized in such a manner that if the stress state is below the yield or failure limit then $F(\sigma_{ij}) < 0$. This implies that if the stress state is above the yield or failure limit then $F(\sigma_{ij}) > 0$. The conditions that $F(\sigma_{ij}) < 0$, $F(\sigma_{ij}) = 0$ and $F(\sigma_{ij}) > 0$ hold when the stress state is below, equal to and above the yield or failure limit respectively, were established in an arbitrary x_i-coordinate system. To make sense they must therefore also hold when we adopt another x_i'-coordinate system. This implies that the value of F is an invariant, i.e.

The yield or failure criterion F is an invariant (8.2)

For anisotropic materials, various expressions of the criterion (8.1) are discussed in Section 8.13. However, we will first consider the important case of isotropic materials.

The stress tensor σ_{ij} can also be expressed by the principal stresses σ_1, σ_2 and σ_3 and the corresponding principal stress directions. As an isotropic material has no directional properties, it is expected that we can write $F = F(\sigma_1, \sigma_2, \sigma_3)$. As the principal stresses are given uniquely in terms of the three stress invariants, we may equally well write F as

$$F(I_1, I_2, I_3) = 0 \tag{8.3}$$

where the 'generic' stress invariants I_1, I_2 and I_3 are defined by

$$I_1 = \sigma_{ii} \; ; \quad I_2 = \frac{1}{2}\sigma_{ij}\sigma_{ji} \; ; \quad I_3 = \frac{1}{3}\sigma_{ij}\sigma_{jk}\sigma_{ki}$$

cf. (3.14). We will now show this result in a more formal manner.

In the x_i-coordinate system, we have $F(\sigma_{ij})$ and if we instead adopt the x_i'-coordinate system, we have $F^*(\sigma_{ij}')$. Since the criterion is an invariant, we conclude that

$$F(\sigma_{ij}) = F^*(\sigma_{ij}') \qquad \text{coordinate invariance} \tag{8.4}$$

This condition is just a result of F being an invariant, i.e. a zero-order tensor. The function F is a response function and in accordance with the discussion following (5.7), the response function is denoted F in the x_i-coordinate system and F^* in the x_i'-coordinate system.

Isotropy means that the response function is the same in all coordinate systems, cf. (5.13). This implies

$$F(\sigma_{ij}') = F^*(\sigma_{ij}') \qquad \text{isotropy} \tag{8.5}$$

Insertion of (8.5) in (8.4) and noting that $\sigma'_{ij} = A_{ik}\sigma_{kl}A_{jl}$, cf. (3.8), we obtain

$$F(\sigma_{ij}) = F(A_{ik}\sigma_{kl}A_{jl}) \qquad \text{coordinate invariance + isotropy} \tag{8.6}$$

and this result shows that F is an isotropic scalar tensor function. Referring to (6.10) and (6.11), the result (8.3) then follows directly.

As already touched upon, instead of (8.3) we may write alternatively

$$\boxed{F(\sigma_1, \sigma_2, \sigma_3) = 0} \tag{8.7}$$

where σ_1, σ_2 and σ_3 are the principal stresses. The principal stresses are invariants, but it is observed that σ_1 is the principal stress in the first principal direction, σ_2 is the principal stress in the second principal direction and σ_3 is the principal stress in the third principal direction. However, since the yield or failure criterion (8.7) only depends on (true) invariants having no directional preferences, the ordering of σ_1, σ_2 and σ_3 i (8.7) is indifferent. That is, (8.7) should be interpreted as a function of principal stresses without any reference to specific principal axes. To emphasize this, we may write (8.7) as

$$F(\sigma_1, \sigma_2, \sigma_3) = F(\sigma_2, \sigma_1, \sigma_3) = F(\sigma_1, \sigma_3, \sigma_2)$$
$$= F(\sigma_3, \sigma_1, \sigma_2) = F(\sigma_3, \sigma_2, \sigma_1) = F(\sigma_2, \sigma_3, \sigma_1) = 0$$

However, if we adopt some convention, for instance that $\sigma_1 \geq \sigma_2 \geq \sigma_3$, the formulation (8.7) suffices.

Determination of the principal stresses requires the solution of an eigenvalue problem and this obstacle is avoided by expressing the criterion in terms of the stress invariants. However, instead of the invariants used in the format (8.3), it turns out to be more convenient to use another set of invariants and write the yield or failure criterion as $F(I_1, J_2, J_3) = 0$ or, even more advantageously, as

$$\boxed{F(I_1, J_2, \cos 3\theta) = 0} \tag{8.8}$$

where

$$J_2 = \frac{1}{2}s_{ij}s_{ji} \; ; \quad \cos 3\theta = \frac{3\sqrt{3}}{2}\frac{J_3}{J_2^{3/2}} \; ; \quad J_3 = \frac{1}{3}s_{ij}s_{jk}s_{ki} \tag{8.9}$$

where s_{ij} is the deviatoric stress tensor, cf. (3.15). The invariant $cos3\theta$ has not been discussed previously, but in a moment we will provide such a discussion. Generally speaking, old criteria use the format (8.7), whereas modern criteria take advantage of the formulation provided by (8.8). One advantage of the format (8.8) is that it separates the influence of the hydrostatic stress I_1 from the influence of the deviatoric stresses expressed by J_2 and $\cos 3\theta$. Moreover, the invariants I_1, J_2 and $\cos 3\theta$ may be given an illuminating geometrical interpretation as shown in a moment.

Identification of failure and initial yield criteria is one of the classical topics in constitutive mechanics and the literature on this subject is therefore very

extensive. The intention of this chapter is not to provide an overview of all the different criteria proposed, but rather to present some main contributions. In addition to being of practical interest, each of the criteria presented therefore involves features not considered by the other criteria dealt with. Thus, the exposition in this chapter aims at a presentation of the mainstream within failure and initial criteria. For further general information, the reader is referred to Chen (1982), Chen and Saleeb (1982), Chen and Han (1988), Desai and Siriwardane (1984), Jeager and Cook (1976), Hill (1950), Mendelsohn (1968), Nadai (1950) and Paul (1968); a very comprehensive review is provided by Yu (2002).

8.1 Haigh-Westergaard coordinate system - Geometrical interpretation of stress invariants

It is evident that (8.7) may be interpreted as a surface in the Cartesian coordinate system with axes σ_1, σ_2 and σ_3 - the so-called *Haigh-Westergaard coordinate system*, cf. Haigh (1920) and Westergaard (1920). Moreover, with this interpretation it will turn out that it is possible to identify certain geometrical quantities related to the stress invariants I_1, J_2 and $\cos 3\theta$.

For this purpose, consider an arbitrary point P with coordinates $(\sigma_1, \sigma_2, \sigma_3)$ in the Haigh-Westergaard coordinate system, cf. Fig. 8.4a). In this stress space, we may identify the unit vector n_i along the space diagonal. This vector is given by

$$n_i = \frac{1}{\sqrt{3}}(1, 1, 1) \tag{8.10}$$

If the stress point is located along the space diagonal, all principal stresses are equal and the space diagonal is therefore called the *hydrostatic axis*.

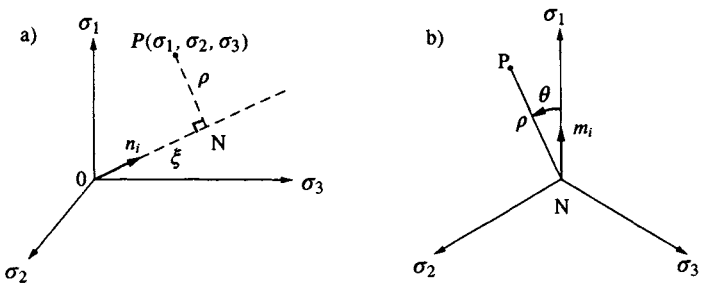

Figure 8.4: a) Haigh-Westergaard coordinate system; b) deviatoric plane perpendicular to the hydrostatic axis and containing line NP.

For any stress point P we may locate a plane which is perpendicular to the hydrostatic axis and which contains the point P. This plane is called the *deviatoric plane* and it contains the line PN in Fig. 8.4a). When viewed in the

direction of the hydrostatic axis, the projections of the σ_1-, σ_2- and σ_3-axes on the deviatoric plane are shown in Fig. 8.4b). The particular deviatoric plane that contains the origin O of the stress space is occasionally called the *π-plane.*

The position of the arbitrary stress point P is given by the Cartesian coordinates $(\sigma_1, \sigma_2, \sigma_3)$. However, instead of these coordinates, we may equally well use the coordinates (ξ, ρ, θ) illustrated in Fig. 8.4. The coordinate ξ is then the distance from the origin O to the point N and ξ is a positive or negative quantity, if the vector $\overline{ON}$ has the same or opposite direction as the unit vector n_i respectively. The coordinate ρ denotes the distance $|\overline{NP}|$ in the deviatoric plane of the point P to the hydrostatic axis. Finally, θ is the angle in the deviatoric plane between the projection of the σ_1-axis on the deviatoric plane and the line NP. It appears that ρ and θ are the polar coordinates of point P in the deviatoric plane.

With this qualitative description, we will now derive explicit expressions for the coordinates (ξ, ρ, θ). From Fig. 8.4a) and (8.10), the coordinate ξ is given by

$$\xi = \boldsymbol{n}^T\overline{OP} = \frac{1}{\sqrt{3}}\begin{bmatrix} 1 & 1 & 1 \end{bmatrix}\begin{bmatrix} \sigma_1 \\ \sigma_2 \\ \sigma_3 \end{bmatrix}$$

i.e.

$$\boxed{\xi = \frac{I_1}{\sqrt{3}}} \tag{8.11}$$

It follows that the vector $\overline{ON} = \xi\mathbf{n}$ is given by

$$\overline{ON} = \frac{I_1}{3}\begin{bmatrix} 1 \\ 1 \\ 1 \end{bmatrix}$$

The vector $\overline{NP}$ in the deviatoric plane then becomes

$$\overline{NP} = \overline{OP} - \overline{ON} = \begin{bmatrix} \sigma_1 \\ \sigma_2 \\ \sigma_3 \end{bmatrix} - \frac{I_1}{3}\begin{bmatrix} 1 \\ 1 \\ 1 \end{bmatrix} = \begin{bmatrix} s_1 \\ s_2 \\ s_3 \end{bmatrix} \tag{8.12}$$

where s_1, s_2 and s_3 are the principal deviatoric stresses. We recall that $\overline{NP}$ is located in the deviatoric plane and since $\overline{NP}$ is given entirely in terms of the deviatoric stresses, this suggests the notation of the deviatoric plane. The length $\rho = \left|\overline{NP}\right|$ of the vector $\overline{NP}$ is given by $\rho^2 = \overline{NP}^T\overline{NP} = s_1^2 + s_2^2 + s_3^2$ i.e.

$$\boxed{\rho = \sqrt{2J_2}} \tag{8.13}$$

where the invariant J_2 is defined by (8.9). It should be observed that, by definition, both ρ and J_2 are non-negative quantities.

With (8.11) and (8.13), we have seen that the coordinates ξ and ρ can be expressed in terms of stress invariants. To obtain an expression for the angle θ, cf. Fig. 8.4b), some further manipulations are necessary.

Referring to Fig. 8.4b), the unit vector m_i located in the deviatoric plane and directed along the projection of the σ_1-axis on the deviatoric plane must have the form

$$m_i = (a, -b, -b)$$

where $a > 0$ and $b > 0$. Since m_i is orthogonal to the hydrostatic axis we have $m_i n_i = 0$, cf. Fig. 8.4, and this leads to $b = a/2$. Moreover, as m_i is a unit vector, we conclude that

$$m_i = \frac{1}{\sqrt{6}}(2, -1, -1) \tag{8.14}$$

The angle θ is measured from the m_i-vector in the counter-clockwise direction towards the vector $\overline{NP}$, i.e. we obtain with (8.12) and (8.14)

$$\rho\cos\theta = \boldsymbol{m}^T\overline{NP} = \frac{1}{\sqrt{6}}\begin{bmatrix} 2 & -1 & -1 \end{bmatrix}\begin{bmatrix} s_1 \\ s_2 \\ s_3 \end{bmatrix} = \frac{2s_1 - s_2 - s_3}{\sqrt{6}}$$

With ρ given by (8.13) and since $s_2 + s_3 = -s_1$ we obtain

$$\cos\theta = \frac{\sqrt{3}}{2}\frac{s_1}{\sqrt{J_2}} \tag{8.15}$$

Use of the trigonometric identity $\cos 3\theta = 4\cos^3\theta - 3\cos\theta$ then results in

$$\cos 3\theta = \frac{3\sqrt{3}}{2J_2^{3/2}}s_1(s_1^2 - J_2) \tag{8.16}$$

To obtain a more convenient expression for $\cos 3\theta$, we shall perform some algebraic manipulations. From the definition of J_2, cf. (8.9), and since $s_1 = -(s_2 + s_3)$ we find

$$s_1^2 - J_2 = \frac{1}{2}(s_1^2 - s_2^2 - s_3^2) = \frac{1}{2}[(s_2 + s_3)^2 - s_2^2 - s_3^2] = s_2 s_3 \tag{8.17}$$

We next note from (3.17) that the invariant J_3 also can be written as

$$J_3 = s_1 s_2 s_3$$

Finally, use of this expression and (8.17) in (8.16) provides the result

$$\boxed{\cos 3\theta = \frac{3\sqrt{3}}{2}\frac{J_3}{J_2^{3/2}}} \tag{8.18}$$

i.e. we have established the relation already stipulated in (8.9) and we have expressed the angle θ in terms of stress invariants. The angle θ is often called the *Lode angle* after Lode (1926). Clearly, the angle θ is also given by (8.15), but the advantage of (8.18) is that here θ is expressed in terms of the stress invariants and not the principal stresses, *per se*. This implies that the eigenvalue problem does not have to be solved as the stress invariants are obtained directly from the stress tensor.

Let us return to the formulation (8.8), i.e.

$$\boxed{F(I_1, J_2, \cos 3\theta) = 0} \tag{8.19}$$

It appears that we have established a very convenient formulation where all the stress invariants can be interpreted geometrically. Moreover, formulation (8.19) separates the influence of the hydrostatic stress I_1 from the influence of the deviatoric stresses as expressed by J_2 and $\cos 3\theta$. Whereas the invariant J_2 tells us about the influence of the magnitude of the deviatoric stresses, cf. (8.13), the invariant $\cos 3\theta$ informs us about the influence of the direction of the deviatoric stresses. In addition, the presence of the term $\cos 3\theta$ enables us to derive a number of symmetry properties of the failure or initial yield criterion, as shown next.

8.2 Symmetry properties of the failure or initial yield curve in the deviatoric plane

It is evident that the failure or initial yield surface intersects the deviatoric plane in a certain curve, cf. Fig. 8.4. It turns out that due to the presence of the term $\cos 3\theta$ in criterion (8.19), we are able to derive a number of general symmetry properties.

Referring to the general criterion (8.19), the trace of this surface with an arbitrary deviatoric plane is obtained for I_1 = constant. As the cos-function is periodic with a period of 360°, we conclude that the failure or yield curve in

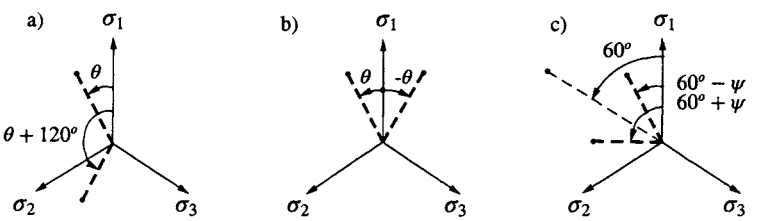

Figure 8.5: General symmetry properties of the failure or initial yield curve in the deviatoric plane; a) 120° period; b) symmetry about $\theta = 0°$; c) symmetry about $\theta = 60°$.

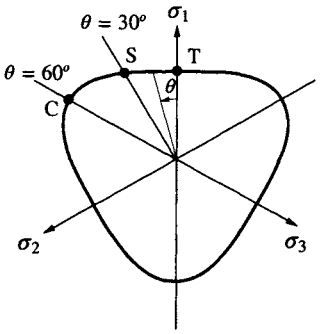

Figure 8.6: Possible shape of failure or initial yield curve in the deviatoric plane. T=tensile meridian, C=compressive meridian, S=shear meridian.

the deviatoric plane is periodic with a period of 120°. That is, the distance ρ, cf. Fig. 8.4b), is the same for θ and for $\theta + 120^o$ as well as for $\theta + 240^o$; this symmetry property is illustrated in Fig. 8.5a). Moreover, as $\cos 3\theta = \cos(-3\theta)$ we find that the curve in the deviatoric plane is symmetric about $\theta = 0^o$; this symmetry property is illustrated in Fig. 8.5b). Due to the periodicity of 120°, the curve is also symmetric about $\theta = 120^o$ and $\theta = 240^o$. Finally, setting $\theta = 60^o + \psi$, i.e. $\psi = 0^o$ corresponds to $\theta = 60^o$, we obtain $\cos 3\theta = -\cos 3\psi$ and setting $\theta = 60^o - \psi$ yields $\cos 3\theta = -\cos 3\psi$. Accordingly, we have the same distance ρ for $\theta = 60^o + \psi$ and $\theta = 60^o - \psi$; it is concluded that the curve in the deviatoric plane is symmetric about $\theta = 60^o$ and thereby also symmetric about $\theta = 180^o$ and $\theta = 300^o$. This symmetry property is illustrated in Fig. 8.5c). In conclusion, the symmetry properties shown in Fig. 8.5 imply that the curve in the deviatoric plane is completely characterized by its form for $0^o \leq \theta \leq 60^o$ and that this shape is repeated in the remaining sectors of the deviatoric plane. We observe that this far-reaching conclusion is a consequence of the material being isotropic.

A possible shape of the failure or initial yield curve in the deviatoric plane fulfilling the above-mentioned 60°-symmetry property is illustrated in Fig. 8.6. Here, the curve is shown as a *convex* curve, a property that does not follow from the mathematical analysis above, but which is strongly confirmed by experimental evidence, irrespective of the material in question.

We found above that the shape of the curve in the deviatoric plane is characterized by its form for $0^o \leq \theta \leq 60^o$ and it may be of interest to identify the corresponding stress range. For this purpose, let us arrange the principal stresses according to

$$\boxed{\sigma_1 \geq \sigma_2 \geq \sigma_3} \tag{8.20}$$

where tension is considered as a positive quantity. This allows us to write

$$\sigma_2 = (1-\alpha)\sigma_1 + \alpha\sigma_3 \; ; \qquad 0 \leq \alpha \leq 1$$

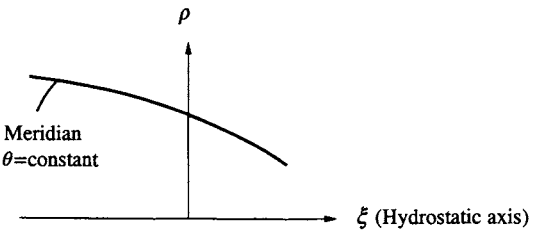

Figure 8.7: Meridian plane obtained by the intersection of the failure or initial yield surface with a plane containing the hydrostatic axis.

i.e.

$$s_1 = \tfrac{1}{3}(1+\alpha)(\sigma_1 - \sigma_3) \;\; ; \;\; s_2 = \tfrac{1}{3}(1-2\alpha)(\sigma_1 - \sigma_3)$$

$$s_3 = -\tfrac{1}{3}(2-\alpha)(\sigma_1 - \sigma_3)$$

With these expressions, (8.15) takes the form

$$\cos\theta = \frac{1+\alpha}{2\sqrt{\alpha^2 - \alpha + 1}} \tag{8.21}$$

For α in the range $0 \leq \alpha \leq 1$, it follows that $0 \leq \theta \leq 60^o$, i.e. with the ordering of the principal stresses given by (8.20), all stress states are covered by the range $0 \leq \theta \leq 60^o$.

The *meridians* of the failure or initial yield surface are the curves where θ =constant applies, i.e. they are obtained by the intersection of the failure or initial yield surface with a plane containing the hydrostatic axis. Meridians may conveniently be depicted in a ξ, ρ-coordinate system or in a $I_1, \sqrt{J_2}$-coordinate system, the so-called *meridian plane*, cf. Fig. 8.7. Three meridians are of particular interest.

If $\sigma_1 > \sigma_2 = \sigma_3$ applies then $\alpha = 1$ and it follows from (8.21) that $\theta = 0^o$. This meridian is termed the *tensile meridian*, as the stress state $\sigma_1 > \sigma_2 = \sigma_3$ corresponds to a hydrostatic stress state superposed by a tensile stress in the σ_1-direction. We have

$$\boxed{\sigma_1 > \sigma_2 = \sigma_3 \quad i.e. \;\; \theta = 0^o \;\; \Rightarrow \;\; tensile\ meridian}$$

Uniaxial tensile stress states are located on the tensile meridian, cf. Fig. 8.8a), and so are biaxial compressive stress states when the two compressive principal stresses are equal.

If $\sigma_1 = \sigma_2 > \sigma_3$ holds then $\alpha = 0$ and (8.21) shows that $\theta = 60^o$. This meridian is termed the *compressive meridian*, as the stress state $\sigma_1 = \sigma_2 > \sigma_3$ corresponds to a hydrostatic stress state superposed by a compressive stress in the σ_3-direction. Consequently

$$\boxed{\sigma_1 = \sigma_2 > \sigma_3 \quad i.e. \;\; \theta = 60^o \;\; \Rightarrow \;\; compressive\ meridian} \tag{8.22}$$

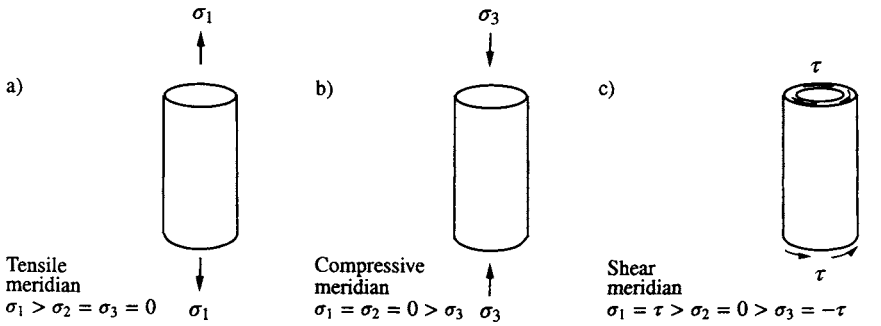

Figure 8.8: Simple examples of stress states located on different meridians; a) uniaxial tension; b) uniaxial compression; c) pure shear.

Uniaxial compressive stress conditions are therefore located on the compressive meridian, cf. Fig. 8.8b).

Finally, if $\sigma_1 > \sigma_2 = (\sigma_1 + \sigma_3)/2 > \sigma_3$ then $\alpha = 1/2$ and it follows from (8.21) that $\theta = 30^o$. This meridian is termed the *shear meridian*, as the stress state $\sigma_1 > \sigma_2 = (\sigma_1 + \sigma_3)/2 > \sigma_3$ corresponds to a hydrostatic stress state superposed by a positive stress, τ, in the σ_1-direction and a negative stress, $-\tau$, in the σ_3-direction. That is

$$\boxed{\sigma_1 > \sigma_2 = \frac{\sigma_1 + \sigma_3}{2} > \sigma_3 \quad i.e. \quad \theta = 30^o \quad \Rightarrow \quad \textit{shear meridian}}$$

A stress state corresponding to pure shear is therefore located on the shear meridian, cf. Fig. 8.8c).

The points where the tensile, compressive and shear meridians intersect the deviatoric plane are illustrated in Fig. 8.6. (Points T, C and S).

To identify points on certain meridians for multiaxial stress states, the *von Kármán pressure cell* is often used, especially for soil and cementitious materials like concrete and rocks. This type of pressure cell is named after von Kármán in recognition of his triaxial tests on marble and sandstone using this kind of equipment, cf. von Kármán (1911). A cylindrical specimen is inserted into a pressure chamber, cf. Fig. 8.9. The oil inside the pressure chamber is pressurized providing stresses on the lateral surface of the specimen and, via a piston, an ordinary testing machine supplies a pressure to the end surfaces of the specimen.

It is evident that the von Kármán pressure cell enables one to test materials along two meridians only: the tensile meridian for which $\sigma_1 > \sigma_2 = \sigma_3$ and the compressive meridian where $\sigma_1 = \sigma_2 > \sigma_3$, cf. Fig. 8.10 (recall that tension is considered as a positive quantity).

Previously, we deduced the general symmetry properties of the curve in the deviatoric plane, cf. Figs. 8.5 and 8.6, and we will now establish some additional symmetry properties which hold under some specialized conditions.

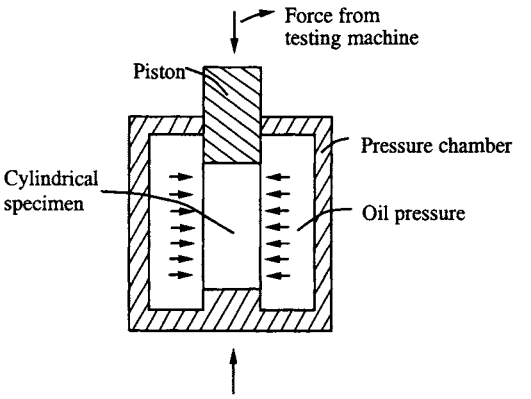

Figure 8.9: Principal sketch of von Kármán pressure cell enabling one to test cylindrical specimens under multiaxial stress states.

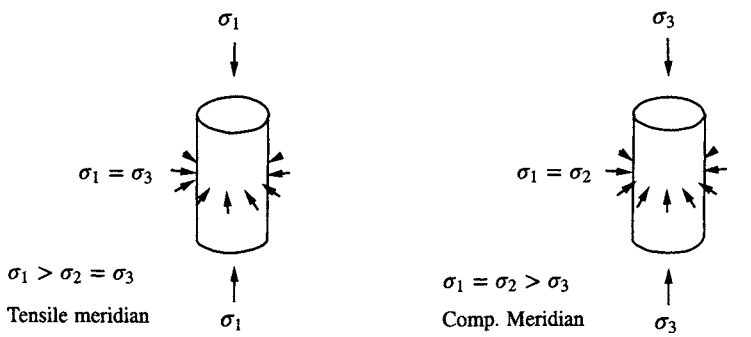

Figure 8.10: Stress states that may be obtained in a von Kármán pressure cell.

Let us assume that the occurrence of failure or initial yield is independent of the hydrostatic stress I_1, i.e. (8.19) reduces to

$$F(J_2, \cos 3\theta) = 0 \tag{8.23}$$

This implies that the corresponding surface in the principal stress space consists of a cylindrical surface with the meridians parallel with the hydrostatic axis. Consequently irrespective of the deviatoric plane considered the same trace of the failure or initial yield surface is obtained. For metals and steel, yielding turns out to be independent of the hydrostatic stress, i.e. (8.23) is a valid assumption.

Let us further assume that criterion (8.23) is fulfilled both for the stress state σ_{ij} and the stress state $-\sigma_{ij}$. As an example, for metals and steel the initial yield stress is the same for uniaxial tension and uniaxial compression. Let us now investigate the consequences of the two assumptions mentioned above. For the stress state σ_{ij}, we may determine J_2, J_3 and thereby $\cos 3\theta$, cf. (8.18).

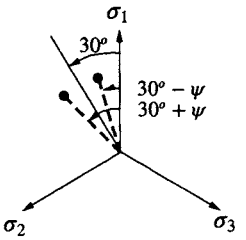

Figure 8.11: Symmetry about $\theta = 30^o$ when (8.23) holds and when σ_{ij} and $-\sigma_{ij}$ both fulfill the criterion.

Likewise, for the stress state $\sigma^*_{ij} = -\sigma_{ij}$, we obtain $J^*_2 = J_2, J^*_3 = -J_3$, i.e. $\cos 3\theta^* = -\cos 3\theta$. This means that for the same J_2–value, criterion (8.23) is fulfilled both for $\cos 3\theta$ and for $-\cos 3\theta$; i.e. both θ as well as $\theta \pm 180^o$ fulfill the criterion. Consider now $\theta = 30^o + \psi$, i.e. $\psi = 0^o$ corresponds to $\theta = 30^o$, cf. Fig. 8.11. We found above that both θ and $\theta - 180^o$ fulfill the criterion; therefore, when $\theta = 30^o + \psi$ fulfills the criterion, so does $\theta = 30^o + \psi - 180^o = -150^o + \psi$. The latter value leads to $\cos 3\theta = \cos(-450^o + 3\psi) = \cos(-90^o + 3\psi) = \cos(90^o - 3\psi)$, which may be interpreted as $\theta = 30^o - \psi$. It is concluded that both $\theta = 30^o + \psi$ and $\theta = 30^o - \psi$ fulfill the criterion and in addition to the general symmetry properties shown in Fig. 8.5, we also have symmetry about $\theta = 30^o$. This symmetry property is illustrated in Fig. 8.11 and it implies that the tensile and compressive meridians have the same distance to the hydrostatic axis.

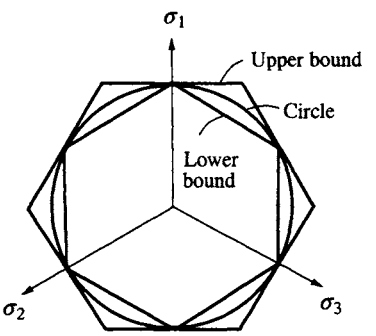

Figure 8.12: Upper and lower bounds for curve in the deviatoric plane when (8.23) holds and when both σ_{ij} and $-\sigma_{ij}$ fulfill the criterion.

The general symmetry properties imply that the curve in the sector $0^o \leq \theta \leq 60^o$ is repeated in the remaining sectors of the deviatoric plane, cf. Fig. 8.6. With the assumptions described above, we also have a symmetry line about $\theta = 30^o$. If we, in addition, assume that the trace in the deviatoric plane is convex – an

assumption that is strongly supported by experimental evidence for all materials – we are led to the upper and lower bounds for the trace in the deviatoric plane as shown in Fig. 8.12.

Let us recall the assumptions that led to these upper and lower bounds. As discussed, these assumptions are in close agreement with the initial yield properties for metals and steel and it is therefore convenient to make the following summation

Initial yield of metals and steel is characterized in that:
* *the hydrostatic stress has no influence*
* *if* σ_{ij} *results in yielding so does* $-\sigma_{ij}$
* *the trace in the deviatoric plane is convex* (8.24)

Recalling that (8.23) implies that the surface in the stress space is a cylindrical surface with the meridians parallel with the hydrostatic axes and observing the upper and lower bounds in the deviatoric plane illustrated in Fig. 8.12, we conclude that there are very narrow bounds within which a valid initial yield criterion for metals and steel can be chosen. Indeed, we shall later see that the circle of Fig. 8.12 corresponds to the *von Mises yield criterion* whereas the lower bound of Fig. 8.12 corresponds to the *Tresca yield criterion.*

Having discussed issues that are of relevance for metals and steel, it may be of interest to evaluate the general experimental evidence for another large group of materials, namely concrete, soil and rocks. These materials are characterized by smooth stress-strain curves exhibiting no well defined initial yield stress. Moreover, the analysis of constructions involving these materials is often focused on the determination of the ultimate load capacity and whereas the ratio $\varepsilon_f/\varepsilon_{yo}$, cf. Fig. 8.2b, is large for metals and steel, it is much smaller for concrete, soil and rocks. For these reasons, the failure criterion is of primary importance for concrete, soil and rocks. Quite generally, the experimental evidence for these materials may be summarized as follows

Failure of concrete, soil and rocks is characterized in that:
* *the hydrostatic stress has a strong influence*
* *inclusion of the term* $\cos 3\theta$ *is of importance*
* *the failure surface is convex* (8.25)

It follows that we expect the failure curve in the deviatoric plane to take the form sketched in Fig. 8.6. We finally observe that experimental observations for cast iron fall somewhere between the characteristics defined by (8.24) and (8.25).

Since elasticity, per definition, only occurs within the initial yield surface, this surface is independent of the previous load history history. On the other hand, to reach the failure surface significant inelastic strains are developed and, in principle, the failure surface is therefore expected to depend on the load history. However, experimental evidence shows for concrete (cf. Chinn and Zimmerman (1965), Schickert and Winkler (1977)), soil (cf. Scott (1963)) and

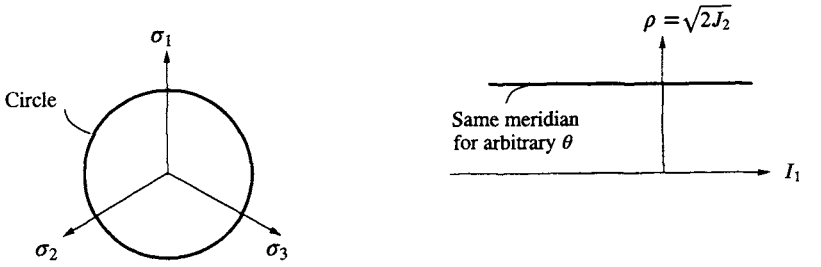

Figure 8.13: von Mises criterion (8.26); a) deviatoric plane; b) meridian plane.

rocks (cf. Swanson and Brown (1971)) that whether the loading is proportional or non-proportional only influences the failure surface to a very modest degree.

8.3 von Mises criterion

For initial yielding of metals and steel, the general experimental evidence is summarized in (8.24). As the hydrostatic stress I_1 has no influence on the yielding, the general criterion (8.19) reduces to (8.23). The simplest assumption is then to ignore the influence of the complicated term $\cos 3\theta$, which leads to $F(J_2) = 0$, i.e. it is assumed that J_2 takes a constant value at yielding, i.e.

$$\sqrt{J_2} - c = 0$$

where c is a constant. This relation may be written in various manners, but the most convenient expression is obtained by

$$\boxed{\sqrt{3J_2} - \sigma_{yo} = 0} \tag{8.26}$$

where, for convenience, the factor 3 in front of J_2 is inserted since $\sqrt{3J_2}$ for uniaxial tension reduces to $\sqrt{3J_2} = \sigma$. According to the criterion, $\sqrt{3J_2}$ takes a constant value for initial yielding and this constant value then becomes σ_{yo}, i.e. the initial yield stress in tension, cf. Fig. 8.1.

Criterion (8.26) is independent of the hydrostatic stress I_1, i.e. it represents a cylindrical surface in the principal stress space with the meridians being parallel with the hydrostatic axis. This means that only the deviatoric stresses influence the criterion. Moreover, it is evident that (8.26) in the deviatoric plane represents a circle, i.e. all meridians are located at the same distance to the hydrostatic axis. These properties are illustrated in Fig. 8.13 and it appears that the circle in the deviatoric plane falls between the lower and upper bounds shown in Fig. 8.12. With these properties, the appearance of the yield surface in the principal stress space takes the form shown in Fig. 8.14.

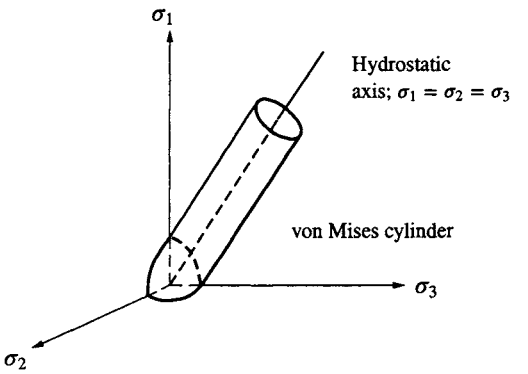

Figure 8.14: von Mises surface in the principal stress space.

The criterion (8.26) was suggested by von Mises (1913) and it is therefore called the *von Mises criterion*; it was anticipated, to some extent, by the proposal of Huber (1904) and the criterion is thus occasionally called the *Huber-von Mises criterion.* Hencky (1924) suggested an interesting physical interpretation of the criterion. Inside the initial yield surface given by (8.26), the material behaves linear elastic. According to (4.95), the strain energy W of a linear elastic and isotropic material can be written as

$$W = W_d + W_v$$

where

$$W_d = Ge_{ij}e_{ij} \; ; \quad W_v = \frac{1}{2}K\varepsilon_{kk}\varepsilon_{mm}$$

It appears that W_d represents the *deviatoric strain energy* whereas W_v is the *volumetric strain energy.* Moreover, as e_{ij} and ε_{kk} are decoupled W_d and W_v are also decoupled. With Hooke's law (4.86) for the deviatoric response, we obtain

$$W_d = \frac{1}{4G}s_{ij}s_{ij} = \frac{1}{2G}J_2$$

i.e. the von Mises yield criterion may be interpreted by saying that initial yield occurs when the deviatoric strain energy achieves a certain value.

Referring to (3.20) the octahedral shear stress τ_o is given by $\tau_o = \sqrt{\frac{2}{3}J_2}$. Another physical interpretation of the von Mises criterion is therefore to claim that the yielding occurs when the octahedral shear stress τ_o that acts on the octahedral plane exceeds a certain value. Expressed in the principal stresses, criterion (8.26) takes the form

$$\boxed{\sqrt{\frac{1}{2}[(\sigma_1 - \sigma_2)^2 + (\sigma_1 - \sigma_3)^2 + (\sigma_2 - \sigma_3)^2]} - \sigma_{yo} = 0} \tag{8.27}$$

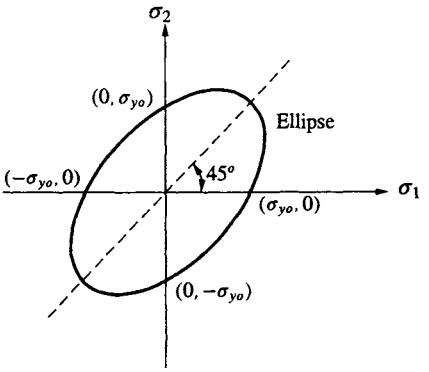

Figure 8.15: von Mises ellipse in the $\sigma_1\sigma_2$–plane.

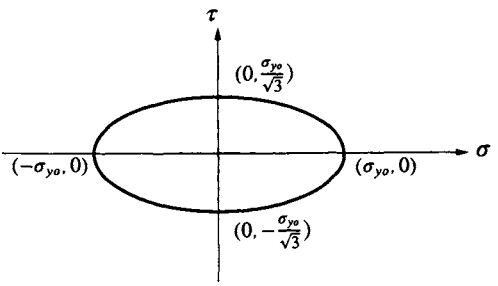

Figure 8.16: von Mises ellipse in the $\sigma\tau$–plane.

For plane stress conditions where $\sigma_3 = 0$ holds, it follows that

$$\sqrt{\sigma_1^2 + \sigma_2^2 - \sigma_1\sigma_2} - \sigma_{yo} = 0 \tag{8.28}$$

which represents an ellipse in the $\sigma_1\sigma_2$-plane as shown in Fig. 8.15. Another stress state of interest is obtained by simultaneous uniaxial stressing and torsion of, for instance, a thin-walled tube. This stress state is given by

$$[\sigma_{ij}] = \begin{bmatrix} \sigma & \tau & 0 \\ \tau & 0 & 0 \\ 0 & 0 & 0 \end{bmatrix} \quad \text{i.e.} \quad [s_{ij}] = \begin{bmatrix} \frac{2}{3}\sigma & \tau & 0 \\ \tau & -\frac{1}{3}\sigma & 0 \\ 0 & 0 & -\frac{1}{3}\sigma \end{bmatrix}$$

We then obtain from (8.26) that

$$\sqrt{\sigma^2 + 3\tau^2} - \sigma_{yo} = 0 \tag{8.29}$$

which represents an ellipse in the $\sigma\tau$–plane, cf. Fig. 8.16. It may be of interest to determine the initial yield shear stress τ_{yo} when $\sigma = 0$ and from (8.29) we

find that

$$\tau_{yo} = \frac{\sigma_{yo}}{\sqrt{3}} \tag{8.30}$$

We have scrutinized the principal ramifications of the von Mises criterion in great detail and in Section 8.8 we will compare its predictions with experimental data for metals and steel.

8.4 Drucker-Prager criterion

We now shift our focus of interest to materials like concrete, soil and rocks. The general failure properties for such materials are summarized in (8.25) and we note that the hydrostatic stress I_1 is of paramount importance. All terms in the general criterion (8.19) must therefore be considered. Even though the term $\cos 3\theta$ is of great importance, this term complicates the criterion considerably; thus we may, as an approximation, simply ignore its influence. We are thereby left with

$$F(I_1, J_2) = 0 \tag{8.31}$$

This formulation was suggested by Schleicher (1926) and (8.31) is often referred to as an *octahedral criterion* since the octahedral normal stress σ_o and the octahedral shear stress τ_o are related to I_1 and J_2 via (3.20), i.e.

$$\sigma_o = \frac{1}{3} I_1 \; ; \quad \tau_o = \sqrt{\frac{2}{3} J_2} \tag{8.32}$$

The simplest possible explicit form of (8.31) is a linear relation between I_1 and $\sqrt{J_2}$, i.e.

$$\boxed{\sqrt{3J_2} + \alpha I_1 - \beta = 0} \tag{8.33}$$

where α and β are material parameters. Moreover, α is dimensionless whereas β has the dimension of stress. The reason for the factor 3 in front of J_2 is that for $\alpha = 0$, (8.33) then reduces exactly to the von Mises criterion (8.26). Criterion (8.33) was suggested by Drucker and Prager (1952) and it is therefore called the *Drucker-Prager criterion.*

Both the octahedral normal stress σ_o and the octahedral shear stress τ_o act on the octahedral plane. Thus, a physical interpretation of the Drucker-Prager criterion is to claim that failure (or yielding) occurs when the octahedral shear stress τ_o exceeds a certain value that depends on the octahedral normal stress.

The deviatoric plane is defined by I_1 = constant, i.e. (8.33) implies that $\sqrt{3J_2}$ is constant in the deviatoric plane. Therefore, the trace in the deviatoric

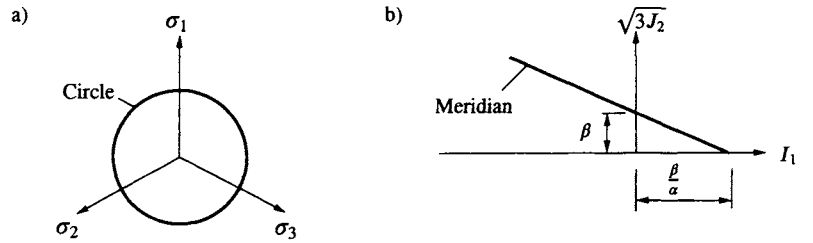

Figure 8.17: Drucker-Prager criterion; a) deviatoric plane; b) meridian plane.

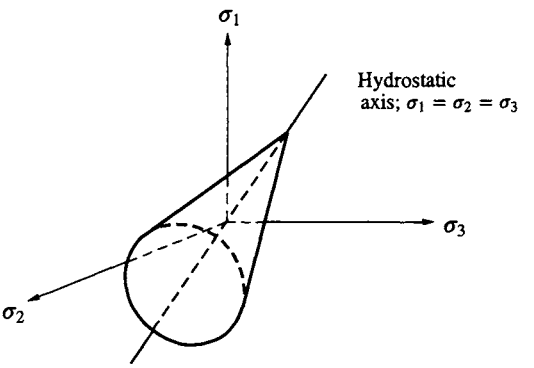

Figure 8.18: Drucker-Prager surface in the principal stress space.

plane is described by a circle. It follows that we have the same meridian irrespective of the θ-angle and that this meridian makes a certain slope with the hydrostatic axis. These features are shown in Fig. 8.17.

Since $\sqrt{3J_2}$ is a non-negative quantity, we conclude from (8.33) with $I_1 = 0$ that β is a positive material parameter. Moreover, as illustrated in Fig. 8.17b) the Drucker-Prager surface intersects the I_1-axis for $I_1 = \beta/\alpha$. Considering failure conditions, it is evident that a material like rock or concrete will break for a sufficiently large hydrostatic tension. Therefore, the dimensionless parameter α must be a non-negative quantity as illustrated in Fig. 8.17b).

In accordance with the properties given by Fig. 8.17, the appearance of the Drucker-Prager criterion in the principal stress space takes the form of a circular cone, as shown in Fig. 8.18.

For plane stress conditions, i.e. $\sigma_3 = 0$, (8.33) reduces to

$$\sqrt{\sigma_1^2 + \sigma_2^2 - \sigma_1\sigma_2} + \alpha(\sigma_1 + \sigma_2) - \beta = 0 \tag{8.34}$$

which obviously reduces to the von Mises expression (8.28) for $\alpha = 0$. As shown in Fig. 8.19, (8.34) represents an off-center ellipse in the $\sigma_1\sigma_2$–plane. The *uniaxial tensile strength* σ_t, *uniaxial compressive strength* σ_c, *biaxial tensile*

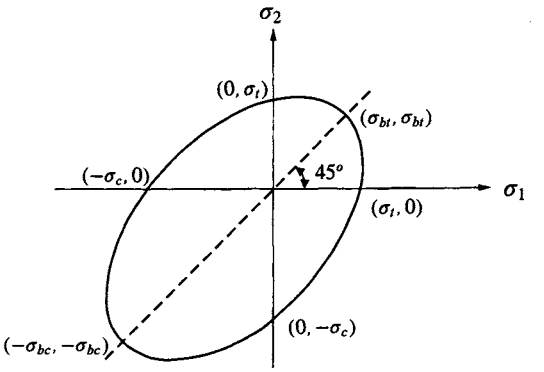

Figure 8.19: Drucker-Prager off-center ellipse in the $\sigma_1\sigma_2$–plane.

strength σ_{bt} and the *biaxial compressive strength* σ_{bc} are illustrated in Fig. 8.19 and from (8.34) we derive that

$$\sigma_t = \frac{\beta}{1+\alpha} \; ; \quad \sigma_c = \frac{\beta}{1-\alpha}$$

and

$$\sigma_{bt} = \frac{\beta}{1+2\alpha} \; ; \quad \sigma_{bc} = \frac{\beta}{1-2\alpha} \tag{8.35}$$

These relations may be used to identify the material parameters α and β.

We will later, in Section 8.10, compare the predictions of the Drucker-Prager criterion with experimental data, but we may already at this state emphasize that due to the elimination of the $\cos 3\theta$-term, the Drucker-Prager criterion should be used with caution. In practice, it can only be used with sufficient accuracy when α is small, i.e. when the influence of the hydrostatic stress I_1 is moderate. Cast iron may be representative of such a material.

8.5 Coulomb criterion

We will again consider failure characteristics for concrete, soil and rocks, but instead of the formulation (8.19), we will adopt the description given by (8.7), i.e.

$$F(\sigma_1, \sigma_2, \sigma_3) = 0 \tag{8.36}$$

with the convention that

$$\boxed{\sigma_1 \geq \sigma_2 \geq \sigma_3}$$

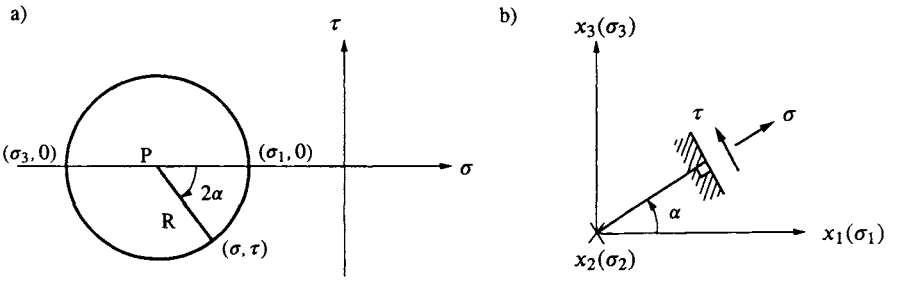

Figure 8.20: a) Mohr's circle of stress; b) corresponding interpretation of σ and τ.

In general, (8.36) is quite complicated and in order to simplify the expression, it is tempting to assume that the intermediate principal stress σ_2 is of minor importance, i.e. we assume that

$$F(\sigma_1, \sigma_3) = 0$$

The most simple expression of this form is then provided by a linear relation between σ_1 and σ_3, i.e.

$$k\sigma_1 - \sigma_3 - m = 0 \tag{8.37}$$

where k and m are material parameters. Requiring that this expression should predict the uniaxial compressive strength value σ_c, the stress state $(\sigma_1, \sigma_2, \sigma_3) = (0, 0, -\sigma_c)$ should fulfill (8.37) and we find

$$\boxed{k\sigma_1 - \sigma_3 - \sigma_c = 0} \tag{8.38}$$

This so-called *Coulomb criterion* was suggested by Coulomb (1776) and is the oldest criterion ever proposed.

To comply with the present exposition, we have here chosen to derive the Coulomb criterion from (8.36), but traditionally the Coulomb criterion is established in a different manner. As this traditional establishment makes for some interesting interpretations, we will now form a bridge between the two viewpoints.

Following Section 3.5, Mohr's circle of stress is shown in Fig. 8.20a). In Fig. 8.20b), the x_1, x_2, x_3–coordinate system is collinear with the principal directions of σ_1, σ_2 and σ_3 and the interpretation of the stress point (σ, τ) in Fig. 8.20a) is shown in Fig. 8.20b). That is, the normal stress σ and the shear stress τ act on the section having a normal which makes the angle α with the σ_1–direction. From Fig. 8.20a), the center position P and the radius R of Mohr's circle are given by

$$P = \frac{1}{2}(\sigma_1 + \sigma_3) \; ; \quad R = \frac{1}{2}(\sigma_1 - \sigma_3) \tag{8.39}$$

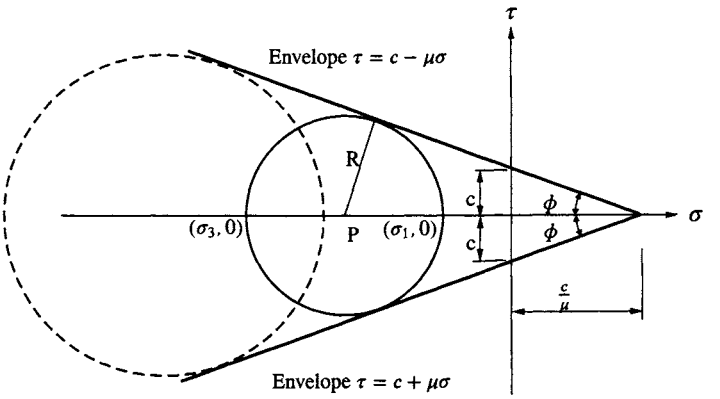

Figure 8.21: Coulomb criterion in Mohr diagram.

It is assumed that the stress state fulfills Coulomb's criterion. Therefore, insertion of σ_3 as determined by (8.38) into (8.39) yields

$$P = \frac{1}{2}[(k+1)\sigma_1 - \sigma_c] \; ; \quad R = \frac{1}{2}[\sigma_c - (k-1)\sigma_1]$$

and elimination of σ_1 provides

$$R = \frac{\sigma_c}{k+1} - \frac{k-1}{k+1}P$$

Thus, the radius R varies linearly with the center position P. Consequently, and as shown in Fig. 8.21, all Mohr's circles of stress that fulfill the Coulomb criterion have two symmetrically positioned straight lines as their envelopes. These straight lines can be written as

$$\boxed{|\tau| = c - \mu\sigma} \tag{8.40}$$

where c and μ are non-negative material parameters. It appears that (8.40) provides an alternative formulation of the Coulomb criterion.

Referring to Fig. 8.21 and (8.40), we see that $|\tau| = c$ is the shear strength when the normal stress $\sigma = 0$, i.e. c is the *cohesion* of the material. If σ is negative, i.e. σ corresponds to a pressure, it follows that the shear strength $|\tau|$ is increased and μ is therefore called the *friction coefficient* of the material. Conseqently, we have obtained a direct physical interpretation of the Coulomb criterion and, most frequently, this criterion is postulated directly in the form given by (8.40).

With this discussion, it is no surprise that the linear expression (8.40) may be generalized to achieve

$$\boxed{|\tau| = h(\sigma)} \tag{8.41}$$

where $h(\sigma)$ denotes an arbitrary function of σ. This so-called *Mohr criterion* was suggested by Mohr (1900) and it is illustrated in Fig. 8.22. Just like the Coulomb criterion, the Mohr criterion (8.41) serves as the envelope of all Mohr's circles of stress when the material is loaded to failure.

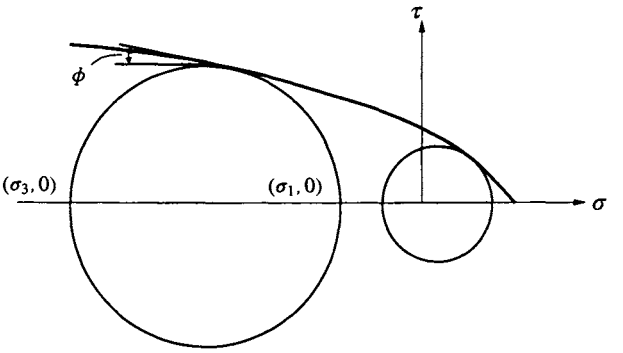

Figure 8.22: Mohr criterion; illustration of current friction angle ϕ.

Returning to the Coulomb criterion, it is of interest to compare the material parameters k and σ_c in (8.38) with the material parameters c and μ in (8.40). First, we observe from Fig. 8.21 that

$$\boxed{\tan\phi = \mu}$$

where ϕ is termed the *friction angle*. Let us next consider a hydrostatic stress state $(\sigma_1, \sigma_2, \sigma_3) = (\sigma, \sigma, \sigma)$. It follows from (8.38) that $\sigma = \sigma_c/(k-1)$ and from Fig. 8.21, we have $\sigma = c/\mu$. This provides

$$\frac{c}{\mu} = \frac{\sigma_c}{k-1} \tag{8.42}$$

Observing that P for the situation displayed in Fig. 8.21 is a negative quantity, cf. (8.39), we obtain from Fig. 8.21, (8.42) and (8.39) that

$$\sin\phi = \frac{R}{\frac{c}{\mu} - P} = \frac{\frac{1}{2}(\sigma_1 - \sigma_3)}{\frac{\sigma_c}{k-1} - \frac{1}{2}(\sigma_1 + \sigma_3)}$$

i.e.

$$\frac{1+\sin\phi}{1-\sin\phi}\sigma_1 - \sigma_3 - \frac{2\sigma_c}{k-1}\frac{\sin\phi}{1-\sin\phi} = 0$$

A comparison with (8.38) reveals that

$$\boxed{k = \frac{1+\sin\phi}{1-\sin\phi}} \quad i.e. \quad k \geq 1$$

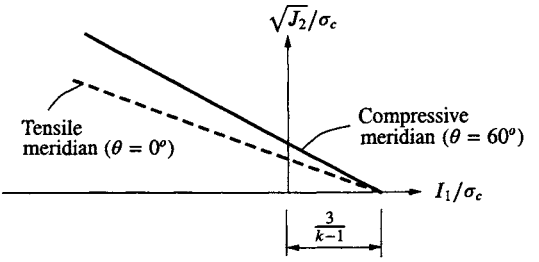

Figure 8.23: Coulomb criterion in meridian plane.

i.e.

$$\sin\phi = \frac{k-1}{k+1} \tag{8.43}$$

As $\tan\phi = \sin\phi/\sqrt{1-\sin^2\phi}$, this implies

$$\boxed{\mu = \tan\phi = \frac{k-1}{2\sqrt{k}}} \tag{8.44}$$

Moreover, this expression and (8.42) yield

$$\boxed{c = \frac{\sigma_c}{2\sqrt{k}}} \tag{8.45}$$

With this discussion of the relations between the various material parameters, we return to the Coulomb criterion given in the form of (8.38). Suppose that the stress state $(\sigma_1, \sigma_2, \sigma_3)$ fulfills the criterion. Let us on this stress state superpose a hydrostatic stress state given by the quantity p; this results in the stress state $(\sigma_1 + p, \sigma_2 + p, \sigma_3 + p)$. It is evident that this new stress state fulfills criterion (8.38) only if $p(k-1) = 0$, i.e. if $k = 1$. It is concluded that criterion (8.38) depends on the hydrostatic stress state if $k \neq 1$, i.e.

$$\boxed{\begin{array}{l}\textit{The Coulomb criterion (8.38) depends}\\ \textit{on the hydrostatic stress if } k \neq 1\end{array}} \tag{8.46}$$

Criterion (8.38) defines a plane in the principal stress space, i.e. the meridians take the form of straight lines. Moreover, the trace in the deviatoric plane ($0^o \leq \theta \leq 60^o$ corresponding to $\sigma_1 \geq \sigma_2 \geq \sigma_3$) is also a straight line. Let us now scrutinize the compressive and tensile meridians.

Along the compressive meridian ($\sigma_1 = \sigma_2 > \sigma_3$, $\theta = 60^o$), we obtain

$$I_{1c} = 2\sigma_1 + \sigma_3 \quad ; \quad \sqrt{J_{2c}} = \frac{1}{\sqrt{3}}(\sigma_1 - \sigma_3) \tag{8.47}$$

where subscript c refers to the compressive meridian. Expressing σ_1 and σ_3 in terms of I_{1c} and $\sqrt{J_{2c}}$ and insertion into (8.38) result in

$$\sqrt{J_{2c}} + \frac{k-1}{\sqrt{3}(k+2)} I_{1c} - \frac{\sqrt{3}\sigma_c}{k+2} = 0 \tag{8.48}$$

As expected $\sqrt{J_{2c}}$ is independent on the hydrostatic stress when k=1.

Along the tensile meridian ($\sigma_1 > \sigma_2 = \sigma_3$, $\theta = 0^o$), we have

$$I_{1t} = \sigma_1 + 2\sigma_3 \;\; ; \;\; \sqrt{J_{2t}} = \frac{1}{\sqrt{3}}(\sigma_1 - \sigma_3) \tag{8.49}$$

where subscript t refers to the tensile meridian. Expressing σ_1 and σ_3 in terms of I_{1t} and $\sqrt{J_{2t}}$ and insertion into (8.38) provide

$$\sqrt{J_{2t}} + \frac{k-1}{\sqrt{3}(2k+1)} I_{1t} - \frac{\sqrt{3}\sigma_c}{2k+1} = 0 \tag{8.50}$$

Expressions (8.48) and (8.50) are illustrated in Fig. 8.23

To determine the trace in the deviatoric plane, we recall that here $I_1 = I_{1t} = I_{1c}$, i.e. elimination of this quantity from (8.48) and (8.50) yields

$$\frac{\rho_c}{\rho_t} = \frac{\sqrt{2J_c}}{\sqrt{2J_t}} = \frac{2k+1}{k+2} \tag{8.51}$$

where $\rho = \sqrt{2J_2}$, cf. (8.13). Recalling that the trace of the Coulomb criterion in the deviatoric plane is a straight line when $\sigma_1 \geq \sigma_2 \geq \sigma_3$, i.e. $0^o \leq \theta \leq 60^o$, we obtain the result shown in principle in Fig. 8.24.

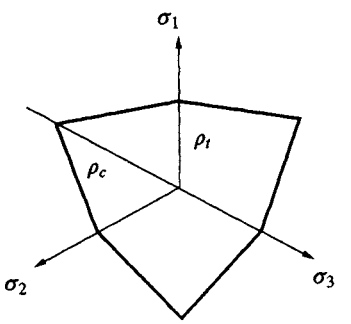

Figure 8.24: Coulomb criterion in the deviatoric plane.

In order to further elucidate the properties of the Coulomb criterion, we consider its predictions for plane stress conditions. From (8.38), the results shown in Fig. 8.25 are easily obtained (note that in this figure the usual convention of

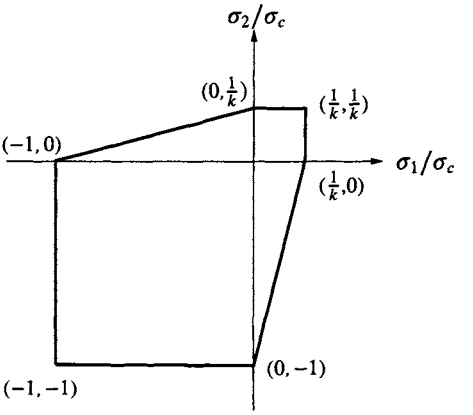

Figure 8.25: Coulomb criterion for plane stress conditions.

$\sigma_1 \geq \sigma_2 \geq \sigma_3$ has been abandoned). It appears that the predicted uniaxial tensile strength becomes $\sigma_t = \sigma_c/k$.

Due to its simplicity, the Coulomb criterion is widely used in analytical applications, cf. for instance Chen (1975) for soil applications and Nielsen (1984) for concrete applications. In numerical applications, however, its use is impeded by the corners of the surface, cf. Fig. 8.24. By calibration of the parameter k, the criterion can be used to model a large variety of material, but, as we will see later, the ignorance of the influence of the intermediate principal stress σ_2 implies that the criterion, in general, will underestimate the experimentally determined failure stresses.

8.6 Mohr's failure mode criterion

We have discussed the assumption of a Coulomb criterion (8.38) or (8.40) in some detail. In this discussion, the Coulomb criterion is simply a criterion that provides information on the magnitude of the failure stresses. Another feature often related to the Coulomb criterion is a *failure mode criterion.* Often in the literature, the failure mode criterion is presented as if it is an integrated part of the Coulomb criterion. We emphasize that this is not the case, as the failure mode criterion is an additional postulate which, in principle, has nothing to do with the failure criterion itself.

The failure mode criterion dates back to Mohr (1900) and it is based on Fig. 8.20b) and the discussion following (8.40). From Figs. 8.20 and 8.21, we may have the situation shown in Fig. 8.26.

Consider the stress state (σ, τ) that satisfies the Coulomb criterion (8.40) in accordance with Fig. 8.26a). From Mohr's circle of stress, the interpretation of σ and τ is displayed in Fig. 8.26b) where the $x_1x_2x_3$-coordinate system is

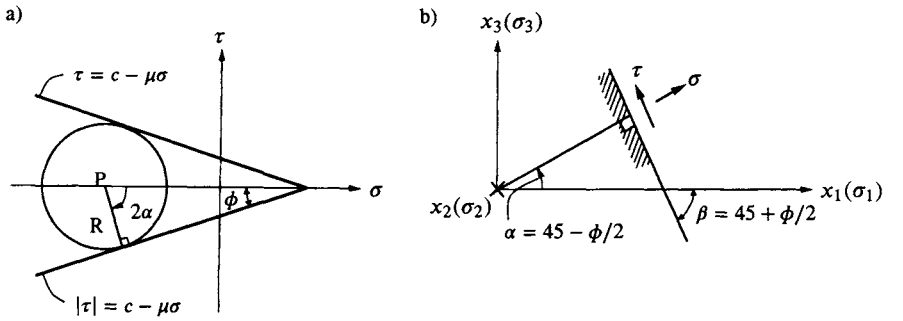

Figure 8.26: a) Coulomb criterion and Mohr's circle; b) interpretation of σ and τ.

collinear with the principal directions of σ_1, σ_2 and σ_3. From Fig. 8.26a) follows that $2\alpha + 90^o + \phi = 180^o$, i.e.

$$\alpha = 45^o - \frac{\phi}{2}$$

It seems tempting to assume that the plane illustrated in Fig. 8.26b) on which the failure stresses σ and τ act is also a *failure plane* where failure takes place in the form of sliding. This plane is also called a *slip plane* since the failure mode is postulated to be a movement along the plane. The angle β which the failure plane makes with the largest principal stress direction (σ_1) becomes $\beta = 45^o + \phi/2$ as shown in Fig. 8.26b).

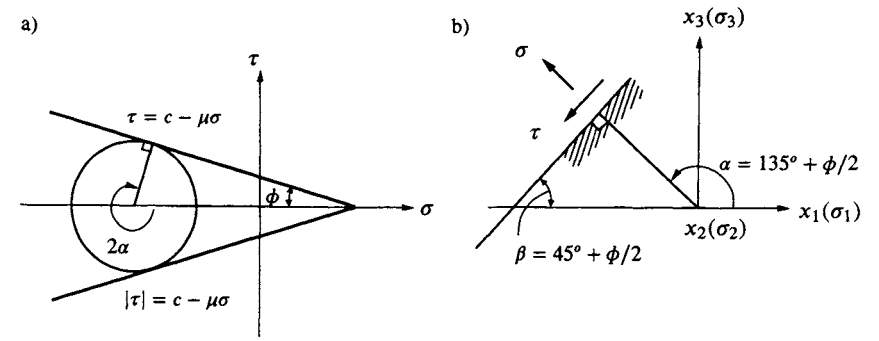

Figure 8.27: a) Coulomb criterion and Mohr's circle; b) interpretation of σ and τ.

Consider next the situation where the stress state (σ, τ) that satisfies the Coulomb criterion is located as displayed in Fig. 8.27a); the corresponding interpretation of σ and τ is shown in Fig. 8.27b). From Fig. 8.27a) follows that $360^o - 2\alpha + 90^o + \phi = 180^o$, i.e.

$$\alpha = 135^o + \frac{\phi}{2}$$

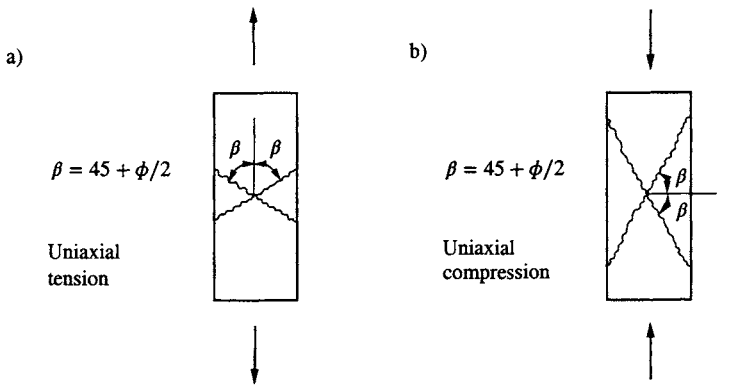

Figure 8.28: Illustration of Mohr's failure mode criterion; a) uniaxial tension; b) uniaxial compression.

Again it is assumed that the plane in Fig. 8.27b) on which the failure stresses σ and τ act is a failure plane. The angle β which this failure plane makes with the largest principal stress direction (σ_1) becomes $\beta = 45^o + \phi/2$ as illustrated in Fig. 8.27b). It is observed that the two failure planes shown in Figs. 8.26b) and 8.27b) both contain the direction of the intermediate principal stress direction (σ_2).

From the discussion above we conclude that

Mohr's failure mode criterion postulates that two failure planes exist. These planes contain the direction of the intermediate principal stress direction and they both make the angle $\beta = 45^o + \phi/2$ with the largest principal stress direction (8.52)

It is emphasized that the angle $\beta = 45^o + \phi/2$ is the angle to the largest principal stress direction (σ_1) and that $\sigma_1 \geq \sigma_2 \geq \sigma_3$, where tension is considered as a positive quantity. From the discussion above follows directly that if a Mohr criterion is used and if ϕ denotes the current friction angle, cf. Fig. 8.22, then conclusion (8.52) also holds. Conclusion (8.52) is illustrated in Fig. 8.28.

It turns out that Mohr's failure mode criterion is often in fair agreement with experimental results for a variety of materials. However, it was emphasized previously that this ingenious failure mode criterion is a postulate and it is of considerable interest that later, in Chapter 24, we will prove that it follows strictly if so-called associated plasticity is adopted whereas so-called non-associated plasticity gives rise to other failure angles.

8.7 Tresca criterion

Let us return to the properties of initial yielding of metals and steel. Referring to (8.24), we recall that the hydrostatic stress has no influence on yielding and we may achieve this property by choosing the parameter $k = 1$ in Coulomb criterion, cf. (8.46). In this case (8.37) reduces to

$$\sigma_1 - \sigma_3 - m = 0 \; ; \quad \sigma_1 \geq \sigma_2 \geq \sigma_3 \tag{8.53}$$

where m is a parameter. Requiring that this expression for uniaxial tension should provide the initial yield stress σ_{yo}, cf. Fig. 8.1, we obtain

$$\boxed{\sigma_1 - \sigma_3 - \sigma_{yo} = 0} \tag{8.54}$$

This so-called *Tresca criterion* was suggested by Tresca (1864) in relation to his work on plastic response of metals. Referring to (3.24), it appears that Tresca's criterion states that the material yields when the maximum shear stress achieves a certain value.

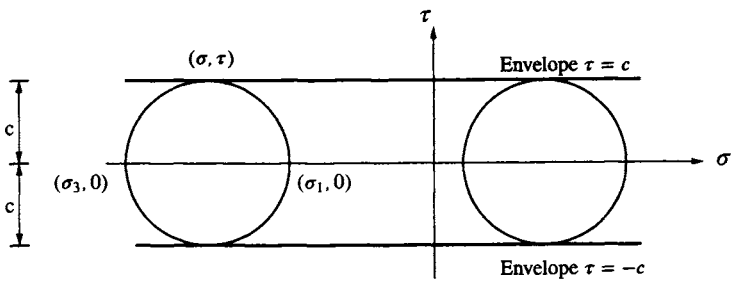

Figure 8.29: Tresca criterion in Mohr diagram.

Since $k = 1$, we conclude from (8.43) and (8.45) that the friction angle ϕ and the cohesion c are given by

$$\boxed{\phi = 0 \; ; \quad c = \frac{\sigma_{yo}}{2}}$$

i.e. in terms of the formulation (8.40), (8.53) is equivalent with

$$\boxed{|\tau| = c}$$

Therefore, in analogy with Fig. 8.21, we achieve the interpretation of this expression as shown in Fig. 8.29

To investigate the Tresca criterion (8.54) in the principal stress space, we obtain from (8.51) and Fig. 8.24 with $k = 1$ that $\rho_t = \rho_c$, i.e. we obtain the trace in the deviatoric plane as shown in Fig. 8.30a). It appears that Tresca's criterion corresponds to the lower bound displayed in Fig. 8.12. Moreover,

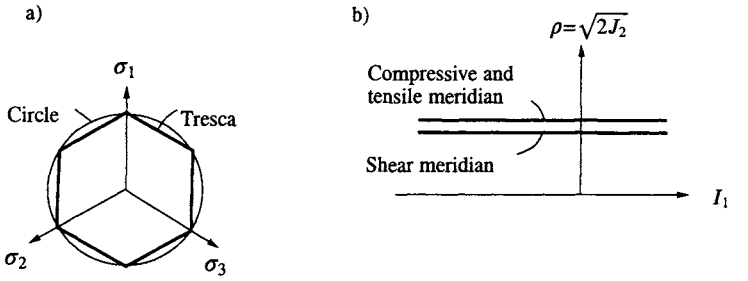

Figure 8.30: Tresca criterion; a) deviatoric plane; b) meridian plane

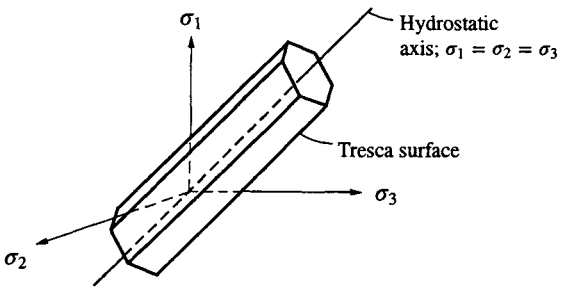

Figure 8.31: Tresca surface in the principal stress space.

from Fig. 8.23 with $k = 1$ the appearance in the meridian plane takes the form shown in Fig. 8.30b.

With these properties the illustration of the yield surface in the principal stress space is given in Fig. 8.31.

For plane stress conditions, (8.54) or Fig. 8.25 with $k = 1$ gives the result illustrated in Fig. 8.32 (note that in this figure the usual convention of $\sigma_1 \geq \sigma_2 \geq \sigma_3$ has been abandoned). This figure may be compared with the corresponding result for the von Mises criterion, cf. Fig. 8.15. Moreover, for simultaneous uniaxial stressing and torsion of, for instance, a thin-walled tube, we have

$$[\sigma_{ij}] = \begin{bmatrix} \sigma & \tau & 0 \\ \tau & 0 & 0 \\ 0 & 0 & 0 \end{bmatrix}$$

Let σ'_{ij} denote the stress components when the coordinate axes are collinear with the principal stress directions, i.e.

$$[\sigma'_{ij}] = \begin{bmatrix} \frac{\sigma}{2} + \frac{1}{2}\sqrt{\sigma^2 + 4\tau^2} & 0 & 0 \\ 0 & 0 & 0 \\ 0 & 0 & \frac{\sigma}{2} - \frac{1}{2}\sqrt{\sigma^2 + 4\tau^2} \end{bmatrix}$$

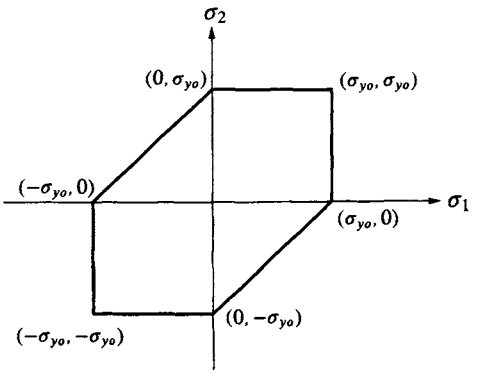

Figure 8.32: Tresca criterion for plane stress conditions.

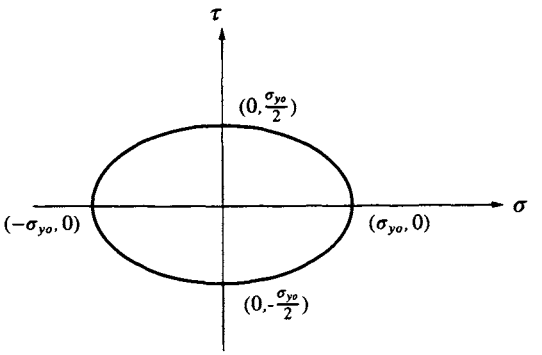

Figure 8.33: Tresca ellipse in the $\sigma\tau$-plane.

From this expression and (8.54) we obtain

$$\sqrt{\sigma^2 + 4\tau^2} - \sigma_{yo} = 0 \tag{8.55}$$

which represents an ellipse in the $\sigma\tau$–plane, cf. Fig. 8.33. Expression (8.55) may be compared with the corresponding result (8.29) using the von Mises criterion. From (8.55) with $\sigma = 0$, the initial yield shear stress becomes

$$\tau_{yo} = \frac{\sigma_{yo}}{2} \tag{8.56}$$

As this shear stress is located along the shear meridian and as the maximum deviation between the von Mises criterion and the Tresca criterion occurs along this meridian, cf. Fig. 8.30a), a comparison between (8.30) and (8.56) reveals that any Tresca yield stress, at most, is 13.4% lower than the corresponding von Mises yield stress.

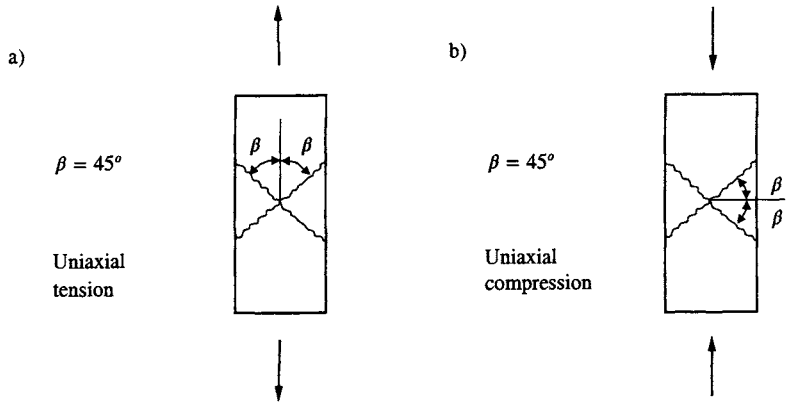

Figure 8.34: Mohr's failure mode criterion for Tresca yielding; a) uniaxial tension; b) uniaxial compression.

Since the friction angle $\phi = 0$ for Tresca's criterion, Mohr's failure mode criterion (8.52) states that any failure plane (slip plane) makes 45^o with the maximum principal stress direction. This is illustrated in Fig. 8.34 and this prediction is in close agreement with experimental results for metals and steel.

8.8 Experimental results for metals and steel – von Mises versus Tresca

We have discussed the principal properties of different criteria in great detail, so it is timely to compare their predictions with experimental results. For this purpose, we will first concentrate on initial yielding of metals and steel. Later, in Sections 8.10 and 8.12, we will focus on failure stresses for concrete and, taken together, these comparisons will provide important information on how different materials behave. As a result, they will enable the reader to get a grasp of the accuracy that may be obtained using different criteria.

For initial yielding of metals and steel, we have already summarized the general experimental evidence in (8.24). Moreover, in relation to Figs. 8.12, 8.13 and 8.30 it can then be argued that Tresca's criterion must provide a lower bound whereas the von Mises criterion is located between the lower and upper bound. We also found that any Tresca yield stress, at most, is 13.4% lower than the corresponding von Mises yield stress. Let us now investigate whether these conclusions are in accordance with experimental data.

It was claimed that initial yielding of metals and steel is independent of the hydrostatic stress I_1. According to the extensive test series of Bridgman (1952), this assumption is closely fulfilled when $|I_1| \leq$ about $4\sigma_{yo}$, i.e. for all cases of

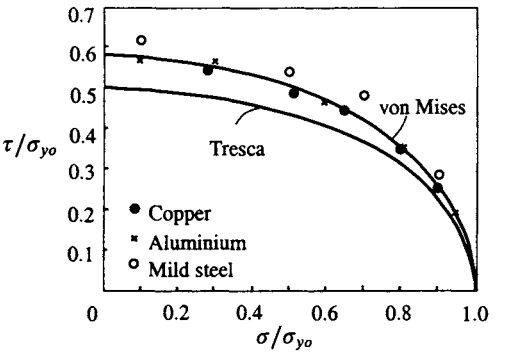

Figure 8.35: Experimental results of Taylor and Quinney (1931).

practical interest. The next issue mentioned in the summary (8.24) is that if the stress state σ_{ij} results in initial yielding so does the stress state $-\sigma_{ij}$. Also this assumption is closely fulfilled and as an example, the initial yield stress is the same for uniaxial tension and uniaxial compression. The last issue mentioned in (8.24) is the convexity of the yield surface and we will see that this assumption is also closely fulfilled.

The classical results of Taylor and Quinney (1931) shown in Fig. 8.35 were obtained by subjecting thin-walled tubes to combined tension and torsion. The figure also shows the ellipses of von Mises and Tresca in accordance with (8.29) and (8.55) and it appears that the von Mises criterion fits the experimental data considerably better than the Tresca criterion.

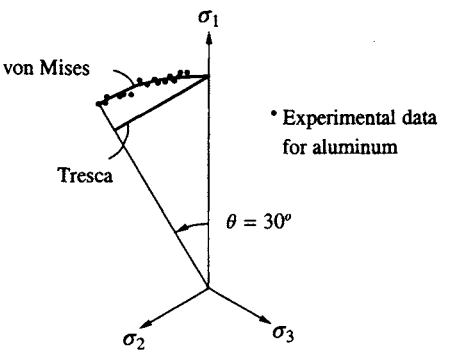

Figure 8.36: Deviatoric plane; experimental data of Lianis and Ford (1957).

The same conclusion may be drawn from the experimental results of Lianis and Ford (1957). They tested commercially pure aluminum specially treated so that a well defined yield stress is obtained. They used a specially designed

notched specimen whereby arbitrary uniform states of combined stresses can be produced; the results are illustrated in the deviatoric plane in Fig. 8.36 together with the predictions of von Mises and Tresca. This figure also demonstrates the convexity of the yield surface.

It is concluded that the general experimental evidence summarized in (8.24) is well-founded and that the von Mises criterion fits the experimental data very closely and it should therefore, in general, be preferred as compared with the Tresca criterion.

8.9 Rankine criterion and modified Coulomb criterion

For brittle materials like concrete and rocks, the Coulomb criterion (8.38) is often used and the parameter k may be fitted to obtain a close agreement with experimental failure stresses for compressive stresses. As an example, in the next section we will see that $k \approx 4$ provides a good approximation for concrete. However, from Fig. 8.25 the Coulomb criterion is seen to predict a uniaxial tensile strength σ_t equal to σ_c/k, i.e. $\sigma_t \approx 0.25\,\sigma_c$ for concrete. This value is far too large for concrete where typical values for σ_t amounts to 5–12 % of the uniaxial compressive strength σ_c.

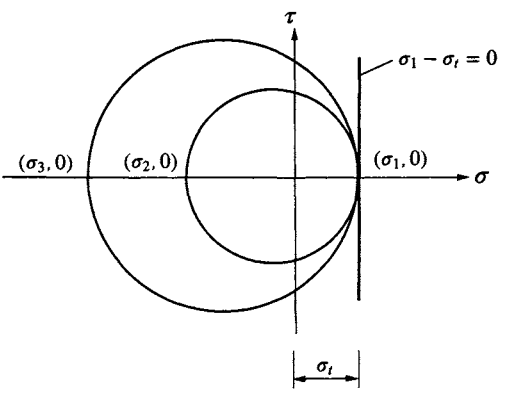

Figure 8.37: Rankine criterion viewed as a Coulomb criterion with the friction angle $\phi = 90^o$.

To remedy this deficiency one may assume a failure criterion in the form

$$\boxed{\sigma_1 - \sigma_t = 0\,; \qquad \sigma_1 \geq \sigma_2 \geq \sigma_3} \tag{8.57}$$

This so-called *Rankine criterion* was proposed by Rankine (1858) and, for obvious reasons, it is occasionally referred to as the *maximum principal stress criterion.* In a Mohr diagram, (8.57) takes the form shown in Fig. 8.37 and it is evident that (8.57) may be viewed as the envelope of all Mohr's stress circles

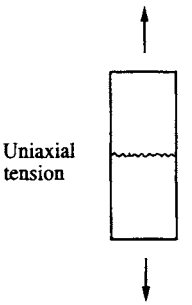

Figure 8.38: Mohr's failure mode criterion for Rankine failure.

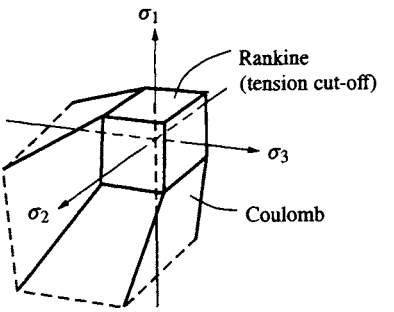

Figure 8.39: Modified Coulomb criterion in the principal stress space.

for which the stress state fulfills (8.57). That is, (8.57) may be viewed as a Coulomb criterion where the friction angle ϕ is given by

$$\boxed{\phi = 90^o} \tag{8.58}$$

cf. Fig. 8.21.

With (8.58) and Mohr's failure mode criterion (8.52) we obtain the failure plane for uniaxial tension as shown in Fig. 8.38; only one failure plane exists and it is perpendicular to the maximum principal stress direction. This result is in close agreement with experimental results for concrete and rocks where the failure manifests itself as a crack perpendicular to the maximum principal stress direction.

Let us return to the Coulomb criterion and its prediction given by Fig. 8.25. To remedy the too high uniaxial tensile strength predicted by the Coulomb criterion, we may use a combined failure criterion which states that failure is obtained, if

$$\boxed{k\sigma_1 - \sigma_3 - \sigma_c = 0 \quad \text{or} \quad \sigma_1 - \sigma_t = 0} \tag{8.59}$$

is fulfilled. This is the *modified Coulomb criterion* which due to its simplicity often is used in analytical calculations, cf. Nielsen (1984).

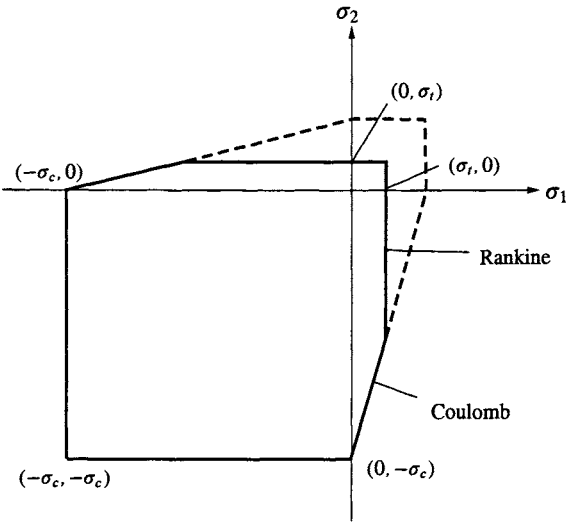

Figure 8.40: Modified Coulomb criterion for plane stress conditions.

Often the Rankine criterion in (8.57) is called a *tension cut-off criterion* and the appearance of the modified Coulomb criterion in the principal stress space is shown in Fig. 8.39. For biaxial stress states the modified Coulomb criterion is illustrated in Fig. 8.40.

8.10 Experimental results for concrete versus the modified Coulomb criterion

The predictions of the modified Coulomb criterion (8.59) will now be compared with experimental failure results for concrete. In this comparison we will adopt

$$k = 4\,; \quad \text{i.e.} \quad \phi = 36.9^o$$

where the friction angle ϕ was determined using (8.44).

Figure 8.41 shows the comparison along the compressive and tensile meridians for stresses ranging from tensile to very large triaxial compressive stresses. It appears that the modified Coulomb criterion provides a fair estimate.

For biaxial stress conditions, the modified Coulomb criterion is compared with the experimental results of Kupfer *et al.* (1969) in Fig. 8.42. Just like in Fig. 8.41, the modified Coulomb criterion underestimates the experimental results. It seems like the modified Coulomb criterion for stresses of most practical interest provides predictions which deviate up to 30% from the correct ones.

It appears that Figs. 8.41 and 8.42 confirm the general experimental evidence for concrete, soil and rocks already summarized in (8.25). There it was stated

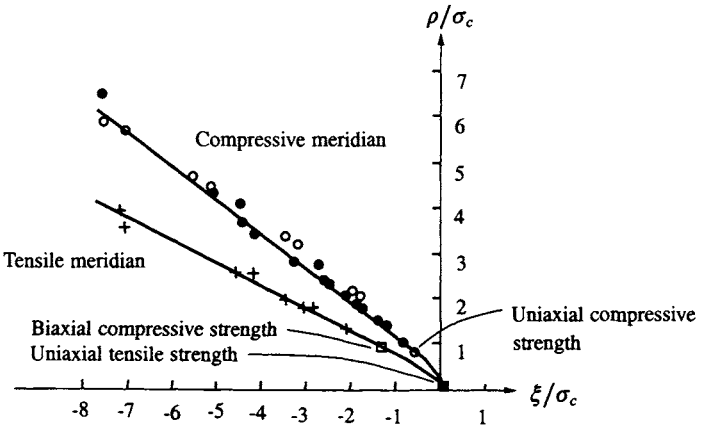

Figure 8.41: Modified Coulomb compared with experimental data in the meridian plane. Along compressive meridian: Balmer (1949)∘, Richart *et al.* (1928)•; along tensile meridian: Richart *et al.* (1928)+, Kupfer *et al.* (1969)□. Moreover, $\sigma_t = 0.08\sigma_c$ is assumed.

that inclusion of the term $\cos 3\theta$ in the failure criterion is of importance. This conclusion is evident from Fig. 8.41 and to substantiate this observation, we may adopt the Drucker-Prager criterion, which lacks the influence of the angle θ, cf. (8.33). Assume that the parameters α and β in (8.33) are calibrated along the compressive meridian. Along this meridian (8.47) holds and insertion into (8.33) yields

$$\frac{1+2\alpha}{1-\alpha}\sigma_1 - \sigma_3 - \frac{\beta}{1-\alpha} = 0$$

If the Coulomb criterion and the Drucker-Prager criterion are calibrated so that they coincide along the compression meridian, a comparison with (8.59) reveals that

$$k = \frac{1+2\alpha}{1-\alpha}; \qquad \sigma_c = \frac{\beta}{1-\alpha}$$

i.e.

$$\alpha = \frac{k-1}{2+k}; \qquad \beta = \frac{3\sigma_c}{2+k} \tag{8.60}$$

The biaxial compressive strength σ_{bc} is located along the tensile meridian, cf. Fig. 8.41, and σ_{bc} as predicted by the Drucker-Prager criterion is given by (8.35) which together with (8.60) results in

$$\sigma_{bc} = \frac{3\sigma_c}{4-k} \tag{8.61}$$

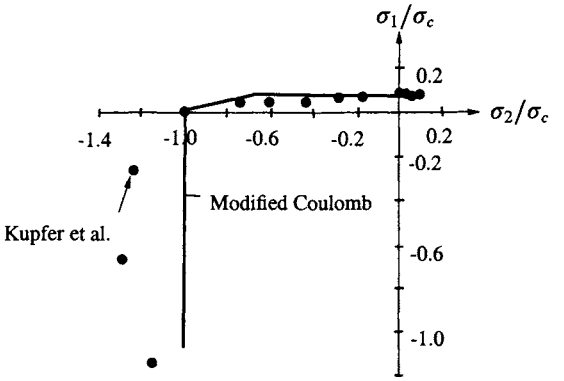

Figure 8.42: Modified Coulomb criterion compared with biaxial test results of Kupfer *et al.* (1969); $\sigma_t = 0.08\sigma_c$ is used.

For concrete $k \approx 4$ and (8.61) shows that if $k \to 4$ then σ_{bc} as predicted by the Drucker-Prager criterion approaches infinity! This surprising result was obtained even though the Drucker-Prager criterion was calibrated to fit the experimental data along the compression meridian closely. Figure 8.42 shows that in reality $\sigma_{bc} \approx 1.2\sigma_c$ and we conclude that the Drucker-Prager criterion should be used with caution. As already stated in Section 8.4, it may only be used with sufficient accuracy when the parameter α is small, i.e. when the influence of the hydrostatic stress I_1 is moderate. Cast iron may be representative of such a material.

8.11 4-parameter criterion

Concerning failure of concrete and rocks, we have discussed the (modified) Coulomb criterion and the Drucker-Prager criterion. The Coulomb criterion lacks the influence of the intermediate principal stress σ_2 and the surface in the principal stress space possesses sharp corners. On the other hand, the Drucker-Prager criterion lacks the influence of the $\cos 3\theta$-term. We will now discuss a criterion which avoids these deficiencies at the expense of a more complicated formulation.

The so-called *4-parameter criterion* was proposed by Ottosen (1977) and it reads

$$\boxed{A\frac{J_2}{\sigma_c^2} + \lambda\frac{\sqrt{J_2}}{\sigma_c} + B\frac{I_1}{\sigma_c} - 1 = 0} \tag{8.62}$$

where the function $\lambda = \lambda(\cos 3\theta)$ is defined by

$$\lambda = \begin{cases} K_1 \cos[\frac{1}{3}\arccos(K_2 \cos 3\theta)] & \text{if} \quad \cos 3\theta \geq 0 \\ K_1 \cos[\frac{\pi}{3} - \frac{1}{3}\arccos(-K_2 \cos 3\theta)] & \text{if} \quad \cos 3\theta \leq 0 \end{cases} \tag{8.63}$$

Moreover, the four dimensionless parameters A, B, K_1 and K_2 are quantities to be determined from experimental evidence. We will require that A, B and K_1 are non-negative quantities and it appears from (8.63) that $0 \leq K_2 \leq 1$, i.e.

$$A \geq 0\,; \quad B \geq 0\,; \quad K_1 \geq 0\,; \quad 0 \leq K_2 \leq 1 \tag{8.64}$$

For reasons that will become apparent later on, K_1 is called a *size factor* whereas K_2 is a *shape factor*. Moreover, it appears from (8.63) and (8.64) that $0 \leq \lambda \leq K_1$.

It follows directly, that (8.62) reduces to the Drucker-Prager criterion (8.33) if $A = K_2 = 0$ and if, in addition, also $B = 0$ we obtain the von Mises criterion (8.26).

The failure surface given by (8.62) intersects the hydrostatic axis only at one point where I_1 takes the positive value given by

$$I_1 = \frac{\sigma_c}{B} \tag{8.65}$$

Moreover, (8.62) shows that the meridians are smooth, convex and curved and to obtain further insight we may solve (8.62) to obtain

$$\frac{\sqrt{J_2}}{\sigma_c} = \frac{1}{2A}\left[-\lambda + \sqrt{\lambda^2 - 4A(B\frac{I_1}{\sigma_c} - 1)}\right] \tag{8.66}$$

As $BI_1/\sigma_c - 1 \leq 0$, cf. (8.65), and as $A \geq 0$ the discriminant of (8.66) is always non-negative. The trace of the failure surface in the deviatoric plane is given by (8.66) for I_1=constant.

If $K_2 = 0$ then λ as given by (8.63) becomes a constant quantity independent of the angle θ. In this case, (8.66) shows that the trace in the deviatoric plane becomes a circle. On the other hand, if $0 < K_2 \leq 1$ then λ depends on the angle θ, i.e. (8.66) shows that also the trace in the deviatoric plane depends on the angle θ. This suggests the terminology of K_2 being a shape factor and it follows directly from (8.63) and (8.66) that K_1 influences the size of the trace in the deviatoric plane.

It is not difficult to prove that if the function $r = 1/\lambda(cos3\theta)$ describes a smooth and convex curve in the polar coordinate system (r, θ), then the trace of the failure surface in the deviatoric plane as given by (8.66) is also a smooth and convex curve; the details of this proof are given by Ottosen (1989).

It is therefore required that the function $r = 1/\lambda(cos3\theta)$ describes a smooth and convex curve in the polar coordinate system (r, θ). The smooth convex contour lines of a deflected membrane loaded by a lateral pressure and supported

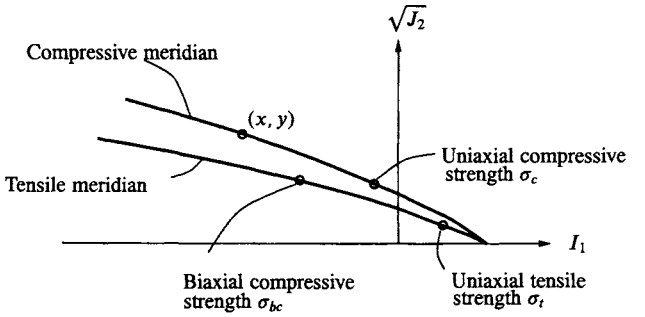

Figure 8.43: Sketch of the four failure states used to calibrate the 4-parameter criterion.

along the edges of an equilateral triangle fulfill these requirements and expression (8.63) was, in fact, derived on this basis. The details of this derivation were given by Ottosen (1975) and they can also be found in Chen (1982).

For the criterion given by (8.62) and (8.63), we have therefore shown that the trace of the failure surface in the deviatoric plane is smooth and convex and thus, it generally takes the form illustrated in Fig. 8.6. We also recall that the meridians are smooth, curved and convex.

To calibrate the four parameters A, B, K_1 and K_2 appearing in (8.62) and (8.63), knowledge of four arbitrary failure stress states is necessary. In practice, the following failure stress states are conveniently used:

1) uniaxial compressive strength σ_c
2) biaxial compressive strength σ_{bc}
3) uniaxial tensile strength σ_t
4) an arbitrary failure state $(I_1, \sqrt{J_2}) = (x, y)$ along the compressive meridian

(8.67)

where we recall that σ_c, σ_{bc} and σ_t are all positive quantities. It appears that failure states 1) and 4) are located on the compressive meridian whereas failure states 2) and 3) are located on the tensile meridian, cf. Fig. 8.43.

Naturally, a numerical approach may be used to determine the four parameters A, B, K_1 and K_2 from the failure states given by (8.67). However, an explicit analytical approach is clearly preferable and in the following we will present such an approach.

Let us first determine the expressions λ_t and λ_c for λ along the tensile and compressive meridian respectively. It follows from (8.63) that

$$\begin{aligned} \lambda_t &= \lambda(\theta = 0^o) = K_1 \cos(\tfrac{1}{3} \arccos K_2) \\ \lambda_c &= \lambda(\theta = 60^o) = K_1 \cos(\tfrac{\pi}{3} - \tfrac{1}{3} \arccos K_2) \end{aligned} \tag{8.68}$$

From the failure states 2) and 3) of (8.67) - both located on the tensile meridian

– use of (8.49) and (8.62) yields

$$\begin{aligned} A\frac{\sigma_{bc}^2}{3\sigma_c^2} + \lambda_t\frac{\sigma_{bc}}{\sigma_c\sqrt{3}} - B\frac{2\sigma_{bc}}{\sigma_c} - 1 = 0 \\ A\frac{\sigma_t^2}{3\sigma_c^2} + \lambda_t\frac{\sigma_t}{\sigma_c\sqrt{3}} + B\frac{\sigma_t}{\sigma_c} - 1 = 0 \end{aligned} \tag{8.69}$$

Likewise, from the failure states 1) and 4) located on the compressive meridian, we find from (8.47) and (8.62)

$$\begin{aligned} \frac{A}{3} + \lambda_c\frac{1}{\sqrt{3}} - B - 1 = 0 \\ A\frac{y^2}{\sigma_c^2} + \lambda_c\frac{y}{\sigma_c} + B\frac{x}{\sigma_c} - 1 = 0 \end{aligned} \tag{8.70}$$

Elimination of λ_t from (8.69) and elimination of λ_c from (8.70) result in the following equations

$$\begin{aligned} A - \frac{9\sigma_c}{\sigma_{bc} - \sigma_t}B = -\frac{3\sigma_c^2}{\sigma_{bc}\sigma_t} \\ -\frac{y}{\sigma_c}A - \kappa B = \sqrt{3} \end{aligned} \tag{8.71}$$

where the dimensionless parameter κ is defined by

$$\boxed{\kappa = \frac{x + y\sqrt{3}}{y - \frac{\sigma_c}{\sqrt{3}}}} \tag{8.72}$$

It appears that κ is a known quantity. Elimination of A from (8.71a) and (8.71b) gives

$$\boxed{B = \frac{\frac{3\sigma_c y}{\sigma_{bc}\sigma_t} - \sqrt{3}}{\kappa + \frac{9y}{\sigma_{bc} - \sigma_t}}} \tag{8.73}$$

Having determined the parameter B, A can be determined from (8.71b), i.e.

$$\boxed{A = -\frac{\sigma_c}{y}(\kappa B + \sqrt{3})}$$

Having determined the parameters A and B, (8.69a) and (8.70a) provide

$$\boxed{\begin{aligned} \lambda_t &= \sqrt{3}\left[\frac{\sigma_c}{\sigma_{bc}} + 2B - \frac{\sigma_{bc}}{3\sigma_c}A\right] \\ \lambda_c &= \sqrt{3}\left[1 + B - \frac{A}{3}\right] \end{aligned}} \tag{8.74}$$

i.e. λ_t and λ_c are now known quantities that, according to (8.68), depend on K_1 and K_2 and thus, the next issue is to determine these parameters.

Define the quantity α by

$$\alpha = \frac{1}{3}\arccos K_2 \tag{8.75}$$

From (8.68) and the relation $\cos(\frac{\pi}{3} - \alpha) = \cos\frac{\pi}{3}\cos\alpha + \sin\frac{\pi}{3}\sin\alpha$, we then obtain

$$\frac{\lambda_t}{K_1} = \cos\alpha\,; \qquad \frac{\lambda_c}{K_1} = \frac{1}{2}\cos\alpha + \frac{\sqrt{3}}{2}\sin\alpha \tag{8.76}$$

Since $\sin\alpha = \pm\sqrt{1 - \cos^2\alpha}$, use of (8.76a) in (8.76b) gives

$$\boxed{K_1 = \frac{2}{\sqrt{3}}\sqrt{\lambda_t^2 + \lambda_c^2 - \lambda_t\lambda_c}} \tag{8.77}$$

where it was used that K_1 is non-negative, cf. (8.64). Since λ_t and λ_c are known also the parameter K_1 can now be determined. From (8.75) follows that $\cos 3\alpha = K_2$ and with the identity $\cos 3\alpha = 4\cos^3\alpha - 3\cos\alpha$ and (8.76a), we conclude that

$$\boxed{K_2 = 4\left(\frac{\lambda_t}{K_1}\right)^3 - 3\frac{\lambda_t}{K_1}} \tag{8.78}$$

From the failure states (8.67), we are therefore able to determine the four parameters A, B, K_1 and K_2 by means of explicit analytical expressions.

As a simple example of the use of these formulas and considering (8.62) and (8.63) as an initial yield criterion, we assume in accordance with experimental evidence for metals and steel that $\sigma_c = \sigma_t = \sigma_{bc} = \sigma_{yo}$. Then (8.73) shows that $B = 0$, i.e. there is no influence of the hydrostatic stress. Expression (8.74) then implies that $\lambda_t = \lambda_c = \sqrt{3}(1 - A/3)$ and we would expect that there is no influence of the angle θ. This is easily verified since (8.77) with $\lambda_t = \lambda_c$ yields $K_1 = 2\lambda_t/\sqrt{3}$, i.e. (8.78) shows that $K_2 = 0$, as expected. Finally, use of $\lambda = \lambda_t = \lambda_c = \sqrt{3}(1 - A/3)$ and $B = 0$ in (8.66) results in

$$\sqrt{J_2} = \frac{\sigma_c}{\sqrt{3}}$$

and we have then recaptured the von Mises criterion, cf. (8.26). In the next section, we shall see some more advanced applications of the calibration formulas derived above.

8.12 Experimental results for concrete versus the 4-parameter criterion

The 4-parameter criterion (8.62) and (8.63) is a very general criterion that can provide close predictions for a variety of materials. In this section we will compare its predictions with experimental failure stresses for concrete.

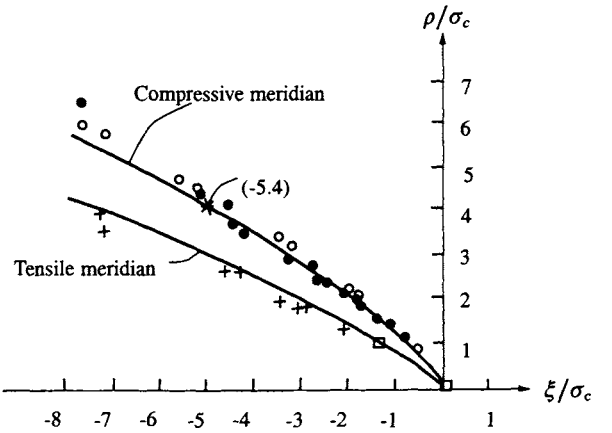

Figure 8.44: 4-parameter criterion compared with experimental data in the meridian plane. Along compressive meridian: Balmer (1949)○, Richart *et al.* (1928)●; along tensile meridian: Richart *et al.* (1928)+, Kupfer *et al.* (1969)□. Moreover, $\sigma_t = 0.10\sigma_c$ is assumed.

To specify the failure states (8.67), we choose

1) uniaxial compressive strength σ_c
2) biaxial compressive strength $\sigma_{bc} = 1.16\,\sigma_c$
3) uniaxial tensile strength $\sigma_t = 0.08\,\sigma_c$, $0.10\,\sigma_c$ and $0.12\,\sigma_c$ (8.79)
4) failure state on the compressive meridian
$(I_1, \sqrt{J_2}) = (x, y) = (\xi\sqrt{3}, \rho/\sqrt{2}) = (-5\sqrt{3}\sigma_c, 4\sigma_c/\sqrt{2})$

Failure state 2) corresponds to the experimental data of Kupfer *et al.* (1969), cf. Fig. 8.42, and the uniaxial tensile strengths given by 3) are typical for concrete. Finally, failure state 4), where relations (8.11) and (8.13) are recalled, is supported by the experimental results shown in Fig. 8.41. With (8.79) and the formulas (8.72) - (8.74), (8.77) and (8.78), the resulting parameter values as well as information of λ_t and λ_c are given in Tables 8.1 and 8.2.

Although the parameters A, B, K_1 and K_2 show considerable dependence on the σ_t/σ_c-ratio, the failure stresses, when only compressive stresses occur, are influenced to a minor extent. Using $\sigma_t/\sigma_c = 0.10$ as a reference, the difference for compressive stresses amounts to less than 2.5 %.

σ_t/σ_c	A	B	K_1	K_2
0.08	1.8076	4.0962	14.4863	0.9914
0.10	1.2759	3.1962	11.7365	0.9801
0.12	0.9218	2.5969	9.9110	0.9647

Table 8.1: Parameter values and their dependence on the σ_t/σ_c– ratio.

σ_t/σ_c	λ_t	λ_c	λ_c/λ_t
0.08	14.4725	7.7834	0.5378
0.10	11.7109	6.5315	0.5577
0.12	9.8720	5.6979	0.5772

Table 8.2: λ_t- and λ_c-values and their dependence on the σ_t/σ_c–ratio.

With these parameter values, the predictions of the 4-parameter criterion are compared with the same experimental data as used in Figs. 8.41 and 8.42. Figure 8.44 shows results along the compressive and tensile meridians and for clarity, the calibration point 4) where $(\xi/\sigma_c,\ \rho/\sigma_c)$ = (-5, 4) is indicated. It may be noted that failure stresses for which $\xi < -5\sigma_c$ are very seldom found in practice and that other experimental data indicates smaller ρ-values in this stress range along the compressive meridian than those shown in Fig. 8.44, cf. Ottosen (1977). For biaxial stress states, a comparison of the predictions and the experimental results of Kupfer *et al.* (1969) is shown in Fig. 8.45. On the whole, Figs. 8.44 and 8.45 show a satisfactory agreement.

The experimental triaxial test results illustrated in Fig. 8.44 are quite old (Richart *et al.* (1928), Balmer (1949)) and especially the failure stresses of Balmer (1949) are larger than other triaxial test data. Thus, it may be of interest to compare the predictions of the 4-parameter criterion with the very accurate triaxial and biaxial results obtained by Schickert and Winkler (1977).

To calibrate the parameters to these data, we now choose the following failure states

$$
\begin{aligned}
&1)\ \text{uniaxial compressive strength } \sigma_c \\
&2)\ \text{biaxial compressive strength } \sigma_{bc} = 1.21\,\sigma_c \\
&3)\ \text{uniaxial tensile strength } \sigma_t = 0.10\,\sigma_c \\
&4)\ \text{failure state on the compressive meridian } (I_1, \sqrt{J_2}) \\
&\quad = (x, y) = (\xi\sqrt{3}, \rho/\sqrt{2}) = (-5\sqrt{3}\sigma_c, 3.28\sigma_c/\sqrt{2})
\end{aligned}
\tag{8.80}
$$

In accordance with the previous discussion, the failure state 4) corresponds to

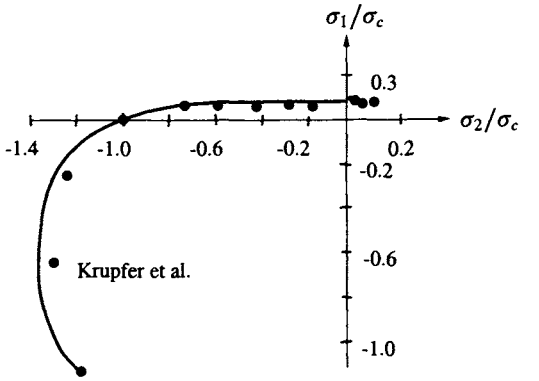

Figure 8.45: 4-parameter criterion compared with biaxial test results of Kupfer *et al.* (1969). Moreover, $\sigma_t = 0.08\,\sigma_c$ is assumed.

A	B	K_1	K_2	λ_c	λ_t	λ_c/λ_t
3.2244	3.4555	11.1538	0.9962	5.8553	11.1491	0.5252

Table 8.3: Parameter values using experimental data of Schickert and Winkler (1977); $\sigma_t/\sigma_c = 0.10$.

somewhat lower failure stresses, cf. (8.79). With (8.80), the parameter values given in Table 8.3 are obtained.

The triaxial results of Schickert and Winkler are of special interest as they were obtained not only along the compressive and tensile meridian, but also along the shear meridian. Moreover, both proportional and non-proportional load paths were used for the triaxial tests and the corresponding effect on the failure stresses may therefore be evaluated. The results of Schickert and Winkler (1977) were presented in terms of octahedral stresses and we recall from (8.32) that $\sigma_o = I_1/3$ and $\tau_o = \sqrt{2J_2/3}$. For triaxial loading, the following four different load paths were used:

* Path 1 : hydrostatic loading until a prescribed σ_o- value.
  This σ_o-value is now held constant and
  τ_o is then increased along the compressive meridian.

* Path 2 : hydrostatic loading until a prescribed σ_o- value.
  This σ_o-value is now held constant and
  τ_o is then increased along the shear meridian.

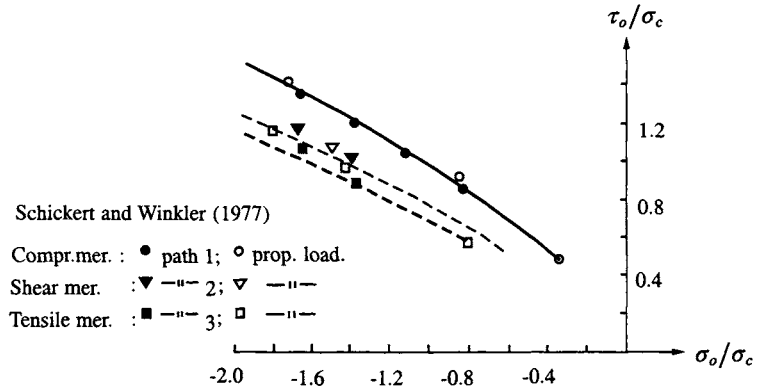

Figure 8.46: 4-parameter criterion compared with experimental data of Schickert and Winkler (1977) in the meridian plane.

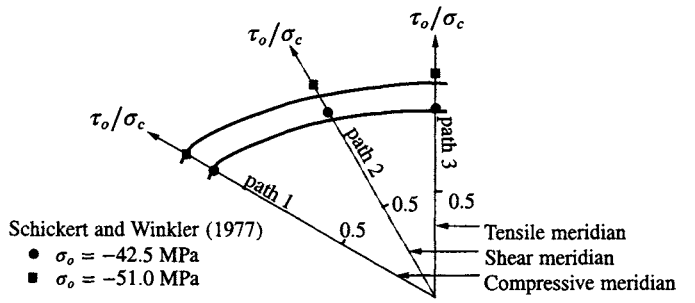

Figure 8.47: 4-parameter criterion compared with experimental data of Schickert and Winkler (1977) in two different deviatoric planes.

* Path 3 : hydrostatic loading until a prescribed σ_o- value. This σ_o-value is now held constant and τ_o is then increased along the tensile meridian.

* Proportional loading along the compressive, shear and tensile meridian.

Figures 8.46 - 8.48 show a comparison of predictions with experimental data. Every experimental point is a mean value based upon three to six tests. The uniaxial compressive strength of the tested concrete is σ_c = 30.6 MPa.

Figure 8.46 shows the compressive, shear and tensile meridians. The agreement along the compressive meridian is close as the (x,y)-value previously discussed was chosen so that deviations were minimized along that meridian. The largest discrepancy amounts to 7 % and occurs along the tensile meridian for large hydrostatic loading.

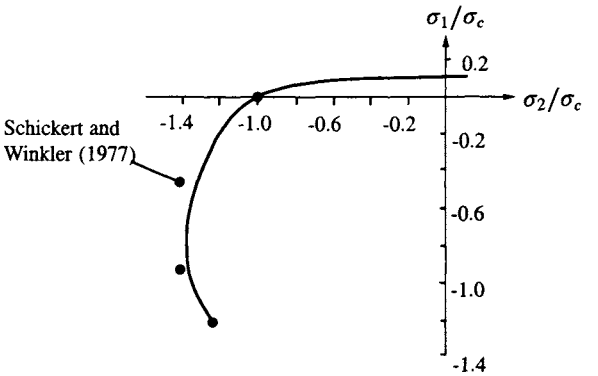

Figure 8.48: 4-parameter criterion compared with biaxial test results of Schickert and Winkler (1977).

Even though the effect is very modest, cf. also the similar observation made by Chinn and Zimmerman (1965), proportional loadings seem to result in higher strengths as compared to non-proportional loadings. The same insignificant tendency is observed for triaxial tests of rocks, cf. Swanson and Brown (1971) and for soil, cf. Scott (1963).

Figure 8.47 shows a comparison in two different deviatoric planes. The largest discrepancy amounts to 5 % and occurs along the shear meridian for large hydrostatic loading. Finally, Fig. 8.48 shows a comparison for biaxial loading. The largest discrepancy amounts to 8 % and occurs for the load path $\sigma_1/\sigma_2 = 1/3$. Based on this extensive comparison with a range of different experimental data, it seems fair to state that it is possible to make close predictions of the failure conditions for general stress conditions. This agreement is in accordance with the general consensus expressed by ASCE (1982), Chen (1982) and Eibl *et al.* (1983) and we may note that the 4-parameter criterion is included in the model code of CEB (Comité Euro-International du Béton) as well as in the Euro-code.

It is observed that other advanced failure criteria for concrete are available that also provide accurate predictions, for instance, the proposals of Hsieh *et al.* (1982), Willam and Warnke (1974) and Podgorski (1985). A detailed description of the first two of these criteria may also be found in Chen (1982). We also refer to the very comprehensive experimental program reported by Gerstle *et al.* (1980)

We finally recall that qualitatively the same features are observed for the failure conditions of concrete, rocks and soil. In that respect, we refer to the failure condition of Krenk (1996) and the proposal of Lade (1977) that is often adopted within soil mechanics.

8.13 Anisotropic criteria

We have presented a rather detailed discussion of concepts and specific criteria for materials that are isotropic. However, many engineering materials are not isotropic and, as examples, we might mention that ice, rolled steel and aluminum exhibit orthotropic properties whereas wood, paper and stratified rocks are strongly orthotropic, cf. the discussion of anisotropy given in Sections 4.3 and 4.6. We will therefore conclude this chapter by a discussion of criteria that account for anisotropic effects. It is emphasized that the intention of this chapter goes beyond a mere presentation of different criteria. Rather, it is to present a mainstream where each of the criteria discussed involves features not covered by the other criteria.

According to (8.2) the yield function is an invariant. For isotropic and anisotropic elasticity, the elastic stiffness tensor D_{ijkl} characterizes the stiffness properties of the material. We may similarly assume that initial yielding for an isotropic or anisotropic material is characterized by the fourth-order tensor P_{ijkl}. The quantity $\sigma_{ij}P_{ijkl}\sigma_{kl}$ is then an invariant and we may then postulate the following criterion

$$\sigma_{ij}P_{ijkl}\sigma_{kl} - 1 = 0 \tag{8.81}$$

If, furthermore, initial yielding is independent of the hydrostatic stress, a valid form of the yield criterion is

$$s_{ij}P_{ijkl}s_{kl} - 1 = 0 \tag{8.82}$$

Depending on the choice of P_{ijkl}, this form can express yielding of various anisotropic materials. As an example, in the extreme case where isotropy is involved, we choose P_{ijkl} as the following isotropic fourth-order tensor

$$P_{ijkl} = \frac{3}{4\sigma_{yo}^2}(\delta_{ik}\delta_{jl} + \delta_{il}\delta_{jk})$$

(8.82) then becomes

$$\frac{3}{2\sigma_{yo}^2}s_{ij}s_{ij} - 1 = 0 \tag{8.83}$$

which is exactly the von Mises criterion, cf. (8.26). With reference to (4.89), the most general isotropic fourth-order tensor P_{ijkl} also includes the term $\delta_{ij}\delta_{kl}$, but since $s_{ii} = 0$ the effect of this term in P_{ijkl} drops out. Written explicitly, (8.83) becomes

$$\frac{1}{2\sigma_{yo}^2}[3s_{11}^2 + 3s_{22}^2 + 3s_{33}^2 + 6s_{12}^2 + 6s_{13}^2 + 6s_{23}^2] - 1 = 0 \tag{8.84}$$

Since $s_{ii} = 0$, we have $3s_{11}^2 = 2s_{11}^2 + s_{11}^2 = 2s_{11}^2 - s_{11}(s_{22} + s_{33})$ as well as $3s_{22}^2 = 2s_{22}^2 - s_{22}(s_{11} + s_{33})$ and $3s_{33}^2 = 2s_{33}^2 - s_{33}(s_{11} + s_{22})$ and (8.84) then takes the following alternative form

$$\frac{1}{2\sigma_{yo}^2}[(s_{11} - s_{22})^2 + (s_{11} - s_{33})^2 + (s_{22} - s_{33})^2 + 6s_{12}^2 + 6s_{13}^2 + 6s_{23}^2] - 1 = 0 \tag{8.85}$$

Let us return to the format (8.81). Changing to a matrix format, it reads

$$\boxed{\boldsymbol{\sigma}^T \boldsymbol{P} \boldsymbol{\sigma} - 1 = 0} \tag{8.86}$$

where $\boldsymbol{\sigma}$ is the column matrix defined by (4.35) and $\boldsymbol{P}$ is a 6×6 matrix. This matrix format is simpler to work with than its tensorial counterpart. However, the price we pay is that (8.86) now refers to a specific coordinate system and proper transformations need to be performed if another coordinate system is chosen. Since the stress components only appear in terms of quadratic expressions, assumption (8.86) implies that if the stress state σ_{ij} results in initial yielding, so does the reversed stress state $-\sigma_{ij}$; for instance, tension and compression in the same direction exhibit the same yield stress. This is a valid assumption for metals and steel.

Suppose that $\boldsymbol{P}$ consists of a symmetric part $\boldsymbol{P}^s$ and an anti-symmetric part $\boldsymbol{P}^a$, i.e. $\boldsymbol{P} = \boldsymbol{P}^s + \boldsymbol{P}^a$, where, according to the definitions of symmetry and anti-symmetry, we have $(\boldsymbol{P}^s)^T = \boldsymbol{P}^s$ and $(\boldsymbol{P}^a)^T = -\boldsymbol{P}^a$. Consider the quantity $b = \boldsymbol{\sigma}^T \boldsymbol{P}^a \boldsymbol{\sigma}$. Since b is a number, we have $b = \boldsymbol{\sigma}^T \boldsymbol{P}^a \boldsymbol{\sigma} = (\boldsymbol{\sigma}^T \boldsymbol{P}^a \boldsymbol{\sigma})^T = \boldsymbol{\sigma}^T (\boldsymbol{P}^a)^T \boldsymbol{\sigma} = -\boldsymbol{\sigma}^T \boldsymbol{P}^a \boldsymbol{\sigma} = -b$ and it is concluded that $b = \boldsymbol{\sigma}^T \boldsymbol{P}^a \boldsymbol{\sigma} = 0$. Without loss of generality, we can therefore take the matrix $\boldsymbol{P}$ in (8.86) to be symmetric, i.e.

$$\boldsymbol{P} = \boldsymbol{P}^T$$

It is concluded that $\boldsymbol{P}$ in the most general case of anisotropy comprises 21 independent components, i.e. 21 material parameters. This is similar to the case when the elastic stiffness $\boldsymbol{D}$ is considered, cf. (4.49).

The anisotropic criterion (8.86) with 21 material parameters for a fully anisotropic material was proposed by von Mises (1928). It seems to be overlooked in the literature that this criterion apparently was the first criterion for anisotropic materials and in a moment we will see that it contains as a special case, a criterion that is often used in practice.

Using the symmetry property of $\boldsymbol{P}$, it can be written as

$$\boldsymbol{P} = \begin{bmatrix} A & -F & -G & P_{14} & P_{15} & P_{16} \\ -F & B & -H & P_{24} & P_{25} & P_{26} \\ -G & -H & C & P_{34} & P_{35} & P_{36} \\ P_{14} & P_{24} & P_{34} & 2L & P_{45} & P_{46} \\ P_{15} & P_{25} & P_{35} & P_{45} & 2M & P_{56} \\ P_{16} & P_{26} & P_{36} & P_{46} & P_{56} & 2N \end{bmatrix} \tag{8.87}$$

where the special notation for the components will turn out to be convenient for later purposes.

Let us split the stress components into a deviatoric part and a hydrostatic part. In matrix notation, this can be written as

$$\boldsymbol{\sigma} = \boldsymbol{s} + \boldsymbol{e} \tag{8.88}$$

where

$$\boldsymbol{\sigma} = \begin{bmatrix} \sigma_{11} \\ \sigma_{22} \\ \sigma_{33} \\ \sigma_{12} \\ \sigma_{13} \\ \sigma_{23} \end{bmatrix}; \quad \boldsymbol{s} = \begin{bmatrix} s_{11} \\ s_{22} \\ s_{33} \\ s_{12} \\ s_{13} \\ s_{23} \end{bmatrix}; \quad \boldsymbol{e} = \frac{1}{3} I_1 \begin{bmatrix} 1 \\ 1 \\ 1 \\ 0 \\ 0 \\ 0 \end{bmatrix} \tag{8.89}$$

Insertion of (8.88) into (8.86) gives

$$\boldsymbol{s}^T \boldsymbol{P} \boldsymbol{s} + (2\boldsymbol{s}^T + \boldsymbol{e}^T)\boldsymbol{P}\boldsymbol{e} - 1 = 0 \tag{8.90}$$

Let us assume that initial yielding of the anisotropic material only depends on the deviatoric stresses; this will be the case, for instance, when considering anisotropic metals and steel. Since the deviatoric part $\boldsymbol{s}$ and the hydrostatic part $\boldsymbol{e}$ can be chosen independent of each other, (8.90) shows that we must require

$$\boldsymbol{P}\boldsymbol{e} = \boldsymbol{0} \tag{8.91}$$

With $\boldsymbol{P}$ and $\boldsymbol{e}$ given by (8.87) and (8.89) respectively, it appears that (8.91) provides 6 equations and the number of independent material parameters has been reduced from 21 to 15 just by requiring yielding to depend on the deviatoric stresses alone. Moreover with (8.91), (8.90) reduces to

$$\boxed{\boldsymbol{s}^T \boldsymbol{P} \boldsymbol{s} - 1 = 0} \tag{8.92}$$

Let us next assume that the material behaves orthotropically with respect to yielding. Previously, we discussed the stiffness matrix $\boldsymbol{D}$ when the material behaves orthotropically, cf. the discussion leading to (4.55). There, orthotropy implies that there exist three planes – so-called elastic symmetry planes – so that $\boldsymbol{D}$ is unchanged for two coordinate systems that are mirror images of each other in these symmetry planes, cf. (4.50). The result of orthotropy, i.e. three elastic symmetry planes, then implies that the matrix $\boldsymbol{D}$ is given by (4.55) where nine independent material parameters exist. In exactly the same manner and considering now orthotropic yield properties, this means that the matrix $\boldsymbol{P}$ is unchanged for two coordinate systems that are mirror images of each other in the three symmetry planes that exist with respect to yielding. While $\boldsymbol{P}$ in the general case is given by (8.87), we conclude that for orthotropy with respect to yielding, and with the symmetry planes being parallel with the coordinate

planes, we require $\boldsymbol{s}'^T\boldsymbol{P}\boldsymbol{s}' = \boldsymbol{s}^T\boldsymbol{P}\boldsymbol{s}$ where $\boldsymbol{s}'$ is related to $\boldsymbol{s}$ by expressions similar to (4.52), (4.54) and (4.56). Trivial calculations show that

$$\boldsymbol{P} = \begin{bmatrix} A & -F & -G & 0 & 0 & 0 \\ -F & B & -H & 0 & 0 & 0 \\ -G & -H & C & 0 & 0 & 0 \\ 0 & 0 & 0 & 2L & 0 & 0 \\ 0 & 0 & 0 & 0 & 2M & 0 \\ 0 & 0 & 0 & 0 & 0 & 2N \end{bmatrix} \tag{8.93}$$

i.e. nine independent materials in complete similarity with (4.55). In order to be as general as possible, we have here distinguished between elastic symmetry planes and the symmetry planes with respect to yielding, but in practice these two sets of planes are expected to coincide.

Since only deviatoric stresses were assumed to influence initial yielding, we have restriction (8.91) which with (8.93) leads to $A = F + G$, $B = F + H$ and $C = G + H$. Thus, we have only six independent material parameters and (8.93) then reduces to

$$\boxed{\boldsymbol{P} = \begin{bmatrix} F+G & -F & -G & 0 & 0 & 0 \\ -F & F+H & -H & 0 & 0 & 0 \\ -G & -H & G+H & 0 & 0 & 0 \\ 0 & 0 & 0 & 2L & 0 & 0 \\ 0 & 0 & 0 & 0 & 2M & 0 \\ 0 & 0 & 0 & 0 & 0 & 2N \end{bmatrix}} \tag{8.94}$$

where F, G, H, L, M and N are material parameters that characterize the orthotropy of the material. Then (8.92) takes the form

$$\boxed{\begin{aligned} &F(s_{11} - s_{22})^2 + G(s_{11} - s_{33})^2 + H(s_{22} - s_{33})^2 \\ &\qquad + 2Ls_{12}^2 + 2Ms_{13}^2 + 2Ns_{23}^2 - 1 = 0 \end{aligned}} \tag{8.95}$$

This is *Hill's orthotropic yield criterion* proposed by Hill (1948a, 1950); a comparison with (8.85) shows that it comprises a generalization of the classical von Mises criterion for anisotropic materials.

To identify the material parameters F, G, H, L, M and N consider the orthotropic material, say wood or rolled steel, illustrated in Fig. 8.49. Here the coordinate axes are aligned with the material axes of orthotropy. Consider a uniaxial stress in the x_1-direction, i.e. $s_{11} = 2\sigma_{11}/3$, $s_{22} = s_{33} = -\sigma_{11}/3$ and $s_{12} = s_{13} = s_{23} = 0$; then (8.95) reduces to

$$(F + G)\sigma_{11}^2 - 1 = 0$$

Let the initial yield stress in the x_1-direction be denoted by σ_{yo}^{11}, then the equation above gives $F + G = 1/(\sigma_{yo}^{11})^2$. Performing the same exercise in the x_2- and

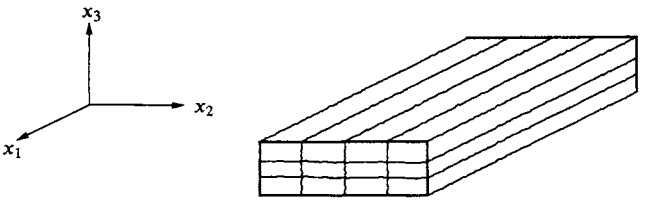

Figure 8.49: Orthotropic material, for instance wood or rolled steel, with coordinate system aligned with the material axes of orthotropy.

x_3-direction, we obtain

$$F+G=\frac{1}{(\sigma_{yo}^{11})^2}\,; \qquad F+H=\frac{1}{(\sigma_{yo}^{22})^2}\,; \qquad G+H=\frac{1}{(\sigma_{yo}^{33})^2}$$

where σ_{yo}^{22} and σ_{yo}^{33} are the initial yield stresses in the x_2- and x_3-direction respectively. From these expressions, we conclude that the parameters F, G and H are determined by

$$\boxed{\begin{aligned} F &= \tfrac{1}{2}\left[\frac{1}{(\sigma_{yo}^{11})^2}+\frac{1}{(\sigma_{yo}^{22})^2}-\frac{1}{(\sigma_{yo}^{33})^2}\right] \\ G &= \tfrac{1}{2}\left[\frac{1}{(\sigma_{yo}^{11})^2}+\frac{1}{(\sigma_{yo}^{33})^2}-\frac{1}{(\sigma_{yo}^{22})^2}\right] \\ H &= \tfrac{1}{2}\left[\frac{1}{(\sigma_{yo}^{22})^2}+\frac{1}{(\sigma_{yo}^{33})^2}-\frac{1}{(\sigma_{yo}^{11})^2}\right] \end{aligned}} \tag{8.96}$$

Let τ_{yo}^{12} denote the initial yield shear stress when the orthotropic material shown in Fig. 8.49 is subjected to the shear stress $\sigma_{12}=s_{12}$; similar notations hold for the initial yield shear stresses τ_{yo}^{13} and τ_{yo}^{23}. Equation (8.95) then leads to

$$\boxed{L=\frac{1}{2(\tau_{yo}^{12})^2}\,; \qquad M=\frac{1}{2(\tau_{yo}^{13})^2}\,; \qquad N=\frac{1}{2(\tau_{yo}^{23})^2}} \tag{8.97}$$

For an isotropic material, (8.96) implies that $F=G=H=1/(2\sigma_{yo}^2)$ and (8.97) gives $L=M=N=1/(2\tau_{yo}^2)$. If, furthermore, $\tau_{yo}=\sigma_{yo}/\sqrt{3}$ then

$$\left.\begin{aligned} F=G=H&=\frac{1}{2\sigma_{yo}^2} \\ L=M=N&=\frac{3}{2\sigma_{yo}^2} \end{aligned}\right\} \quad \Rightarrow \quad \text{von Mises criterion} \tag{8.98}$$

and it appears that (8.95) reduces to the von Mises criterion (8.85).

It is emphasized that (8.95) holds only when the coordinate axes are aligned with the material axes of orthotropy, cf. Fig. 8.49. If this is not the case, the coordinate system must be rotated accordingly and the stress components in the new aligned coordinate system must be determined using (3.8) or (3.9) before use can be made of (8.95).

Hill's criterion (8.95) holds for orthotropic materials, but the degree of orthotropy cannot be arbitrarily large. To identify these restrictions in a rational fashion, we eliminate s_{33} in (8.95) using $s_{33} = -(s_{11} + s_{22})$ to obtain

$$(F + 4G + H)s_{11}^2 + (F + G + 4H)s_{22}^2 + 2(-F + 2G + 2H)s_{11}s_{22} + 2Ls_{12}^2 + 2Ms_{13}^2 + 2Ns_{23}^2 - 1 = 0 \tag{8.99}$$

Here the quantities s_{11}, s_{22}, s_{12}, s_{13} and s_{23} may take arbitrary values independent of each other. If an arbitrary set of s_{11}, s_{22}, s_{12}, s_{13} and s_{23} is increased by a sufficient amount, we must require that it is possible to fulfill (8.99); otherwise there exist arbitrary large deviatoric stress states that do not result in yielding. This is just to say that (8.99) must correspond to a closed surface in the s_{11}, s_{22}, s_{12}, s_{13} and s_{23}-space. Since L, M and N are positive quantities, cf. (8.97), we conclude that increase of the shear stresses will always eventually result in yielding. That is, the quantities that may give rise to restrictions on the degree of orthotropy are related to the first three terms of (8.99). These terms may be written in the following form

$$(F + 4G + H)s_{11}^2 + (F + G + 4H)s_{22}^2 + 2(-F + 2G + 2H)s_{11}s_{22} = \begin{bmatrix} s_{11} & s_{22} \end{bmatrix} \begin{bmatrix} F + 4G + H & -F + 2G + 2H \\ -F + 2G + 2H & F + G + 4H \end{bmatrix} \begin{bmatrix} s_{11} \\ s_{22} \end{bmatrix} \tag{8.100}$$

To avoid the situation that arbitrarily large values of s_{11} and s_{22} will not result in yielding, we must require that the quadratic matrix in (8.100) is positive definite. Thus, the eigenvalues of the matrix must be positive and evaluation of these eigenvalues results in

$$2F + 5(G + H) > 0\,; \qquad F(G + H) + GH > 0$$

From (8.96) appears that the first of these inequalities is always satisfied whereas the second inequality leads to the constraint

$$\boxed{\frac{4}{(\sigma_{yo}^{11})^2(\sigma_{yo}^{22})^2} > \left[\frac{1}{(\sigma_{yo}^{33})^2} - \left(\frac{1}{(\sigma_{yo}^{11})^2} + \frac{1}{(\sigma_{yo}^{22})^2}\right)\right]^2} \tag{8.101}$$

which restricts the applicability range for Hill's criterion.

It may be somewhat surprising that Hill's criterion implies restriction (8.101). However, the key point is that we have assumed the quadratic expression (8.92)

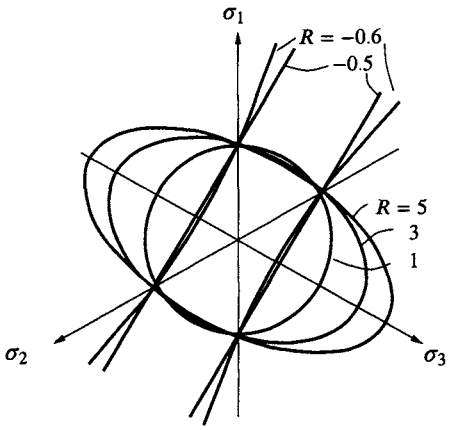

Figure 8.50: Yield curve in deviatoric plane for Hill's criterion; $\sigma_{yo}^{22} = \sigma_{yo}^{11}$, $(\sigma_{yo}^{33})^2 = (\sigma_{yo}^{11})^2\frac{1}{2}(1+R)$ i.e. $R = 1$ corresponds to the von Mises criterion.

and this expression only allows the yield surface to be a closed surface in the deviatoric stress space when (8.101) is fulfilled. To illustrate this aspect, consider a situation where the material axes of orthotropy coincide with the principal stress axes. Then (8.95) - with $s_{12} = s_{13} = s_{23} = 0$ - describes the yield curve in the deviatoric plane. Assume for simplicity that $\sigma_{yo}^{22} = \sigma_{yo}^{11}$. In that case and following Hosford and Backofen (1964), we introduce the dimensionless parameter R to express σ_{yo}^{33} via $(\sigma_{yo}^{33})^2 = \frac{1}{2}(\sigma_{yo}^{11})^2(1+R)$; for $R = 1$, we recover the isotropic case, i.e. the von Mises criterion. Restriction (8.101) then leads to $R > -\frac{1}{2}$, i.e. $\sigma_{yo}^{33} > \frac{1}{2}\sigma_{yo}^{11}$. The yield curves in the deviatoric plane for various R-values are shown in Fig. 8.50 and it appears that when R approaches the limit $R = -\frac{1}{2}$, the trace changes from a closed curve to two parallel lines.

Apart from the classical Hill criterion treated here, we may refer to Hill (1993) for a generalized version; this generalization is widely used and as an example, Tryding (1994) made a calibration applicable to paper.

With this detailed discussion, it is easy to generalize the ideas. In (8.81), P_{ijkl} was assumed to characterize the anisotropy of the material. We may even include the effect of some second-order tensor q_{ij} that also characterizes the anisotropy. Both σ_{ij}, P_{ijkl} and q_{ij} must appear in the form of different combinations of invariants and an evident possibility is

$$\sigma_{ij}P_{ijkl}\sigma_{kl} + \sigma_{ij}q_{ij} - 1 = 0$$

which in matrix notation reads

$$\boxed{\boldsymbol{\sigma}^T\boldsymbol{P}\boldsymbol{\sigma} + \boldsymbol{\sigma}^T\boldsymbol{q} - 1 = 0}$$

where $\boldsymbol{P}$ is a 6x6 matrix and $\boldsymbol{q}$ is a 6x1 column matrix. This is the *Tsai-Wu anisotropic yield criterion* suggested by Tsai and Wu (1971). In this format,

the stress components enter both in quadratic terms and in linear terms, i.e. if the stress state σ_{ij} is located on the yield surface, the reversed stress state $-\sigma_{ij}$ is not; for instance, tension and compression in the same direction exhibit different yield stresses. Moreover, it appears that the effect of the hydrostatic stress is accounted for.

If orthotropy is considered, then a discussion similar to that following (4.52) shows that the $\boldsymbol{q}$-matrix cannot involve components that affect the shear stresses, i.e. $\boldsymbol{q}^T = [q_1\ q_2\ q_3\ 0\ 0\ 0]$. If we, in addition, take the orthotropic $\boldsymbol{P}$-matrix given by (8.94), the Tsai-Wu criterion reduces to the *Hoffman* criterion proposed by Hoffman (1967) which then involves nine independent parameters.

Here, we have concentrated on some classic criteria where the stress components enter via quadratic terms (and linear terms). However, in order to obtain closer fits to experimental data, recent research seems to favor criteria where other powers of the stress components are used. The reader may consult, for instance, Barlat *et al.* (1991) and Karafillis and Boyce (1993) for further information.

We might also mention that calibration of Hoffman's criterion to columnar-grained ice that is orthotropic and where initial yielding depends on the hydrostatic stress is discussed by Chen and Han (1988) and that a further general discussion of anisotropic yield criteria is presented by Rathkjen (1986).

The discussion above has followed a quite classical route and, instead, it may be of interest to pursue the concept provided by structural tensors as discussed in Sections 6.5 and 6.6.

As an illustration, consider orthotropy where we have three orthogonal material directions each identified by the orthogonal unit vectors $\boldsymbol{v}^{(1)}$, $\boldsymbol{v}^{(2)}$ and $\boldsymbol{v}^{(3)}$. In analogy with (6.49) we now define the structural tensors according to

$$\boxed{\boldsymbol{M}^{(1)} = \boldsymbol{v}^{(1)}\boldsymbol{v}^{(1)T};\quad \boldsymbol{M}^{(2)} = \boldsymbol{v}^{(2)}\boldsymbol{v}^{(2)T};\quad \boldsymbol{M}^{(3)} = \boldsymbol{v}^{(3)}\boldsymbol{v}^{(3)T}} \tag{8.102}$$

and from (6.52), we note that

$$\boldsymbol{I} = \boldsymbol{M}^{(1)} + \boldsymbol{M}^{(2)} + \boldsymbol{M}^{(3)} \tag{8.103}$$

Suppose that the coordinate system is chosen collinearly with the material directions. Then we have $\boldsymbol{v}^{(1)T} = [1\,0\,0]$, $\boldsymbol{v}^{(2)T} = [0\,1\,0]$ and $\boldsymbol{v}^{(3)T} = [0\,0\,1]$ and (8.102) becomes

$$\boldsymbol{M}^{(1)} = \begin{bmatrix} 1 & 0 & 0 \\ 0 & 0 & 0 \\ 0 & 0 & 0 \end{bmatrix};\quad \boldsymbol{M}^{(2)} = \begin{bmatrix} 0 & 0 & 0 \\ 0 & 1 & 0 \\ 0 & 0 & 0 \end{bmatrix};\quad \boldsymbol{M}^{(3)} = \begin{bmatrix} 0 & 0 & 0 \\ 0 & 0 & 0 \\ 0 & 0 & 1 \end{bmatrix} \tag{8.104}$$

The yield criterion is now taken as a function of the stresses and the structural tensors. However, since these structural tensors depend on each other through (8.103), we choose to work with $\boldsymbol{M}^{(1)}$ and $\boldsymbol{M}^{(2)}$, only, i.e. $F = F(\boldsymbol{\sigma}, \boldsymbol{M}^{(1)}, \boldsymbol{M}^{(2)})$.

Instead of the coordinate system $\boldsymbol{x}$, we may consider another coordinate system $\boldsymbol{x}'$ where $\boldsymbol{x} = \boldsymbol{A}^T\boldsymbol{x}'$ and $\boldsymbol{A}$ is the orthogonal transformation matrix. If it is assumed that the yield function F is an isotropic scalar tensor function then

$$F(\boldsymbol{\sigma}, \boldsymbol{M}^{(1)}, \boldsymbol{M}^{(2)}) = F(\boldsymbol{A}\boldsymbol{\sigma}\boldsymbol{A}^T, \boldsymbol{A}\boldsymbol{M}^{(1)}\boldsymbol{A}^T, \boldsymbol{A}\boldsymbol{M}^{(2)}\boldsymbol{A}^T) \tag{8.105}$$

for arbitrary $\boldsymbol{A}$ matrices, cf. (6.10). Let S denote the symmetry group in question, i.e. reflections of the coordinate system in the three symmetry planes. For these reflections the structural tensors are unchanged, i.e.

$$\boldsymbol{M}^{(\alpha)} = \boldsymbol{A}\boldsymbol{M}^{(\alpha)}\boldsymbol{A}^T \quad \text{for} \quad \boldsymbol{A} \in S$$

From (8.105), we therefore get

$$F(\boldsymbol{\sigma}, \boldsymbol{M}^{(1)}, \boldsymbol{M}^{(2)}) = F(\boldsymbol{A}\boldsymbol{\sigma}\boldsymbol{A}^T, \boldsymbol{M}^{(1)}, \boldsymbol{M}^{(2)}) \quad \text{for} \quad \boldsymbol{A} \in S$$

That is, for the symmetry group in question, the relation for the yield criterion is as if the material were isotropic, cf (8.6), and this is exactly what is meant by orthotropy.

The representation theorem (6.11) is now applied to $F = F(\boldsymbol{\sigma}, \boldsymbol{M}^{(1)}, \boldsymbol{M}^{(2)})$. The result is completely similar to the discussion in Section 6.5 and in analogy with (6.56) and (6.57) we obtain

$$F = F(I_1, I_2, I_3, I_4, I_5, I_6, I_7) \tag{8.106}$$

where

$$I_1 = tr(\boldsymbol{\sigma}\boldsymbol{M}^{(1)}); \quad I_2 = tr(\boldsymbol{\sigma}\boldsymbol{M}^{(2)}); \quad I_3 = tr(\boldsymbol{\sigma}\boldsymbol{M}^{(3)})$$
$$I_4 = tr(\boldsymbol{\sigma}^2\boldsymbol{M}^{(1)}); \quad I_5 = tr(\boldsymbol{\sigma}^2\boldsymbol{M}^{(2)}); \quad I_6 = tr(\boldsymbol{\sigma}^2\boldsymbol{M}^{(3)}); \quad I_7 = \tfrac{1}{3}tr(\boldsymbol{\sigma}^3)$$

Suppose that we want to derive Hill's criterion; in this criterion, the stress components occur in a quadratic form. In (8.106) we therefore ignore the invariant I_7 and obtain

$$\begin{aligned}\alpha_1(I_1 - I_2)^2 + \alpha_2(I_1 - I_3)^2 + \alpha_3(I_2 - I_3)^2 \\ +\alpha_4(I_4 - I_1^2) + \alpha_5(I_5 - I_2^2) + \alpha_6(I_6 - I_3^2) \\ + \beta_1 I_1 I_2 + \beta_2 I_1 I_3 + \beta_3 I_2 I_3 - 1 = 0\end{aligned} \tag{8.107}$$

where $\alpha_1 \cdots \alpha_6$ and β_1, β_2 and β_3 are constants and where the reason for the specific notation will become evident in a moment. It is observed that (8.107) is the most general quadratic expression that exists and it is an explicit version of the anisotropic von Mises criterion (1928) applicable to orthotropic materials, cf. (8.81) and (8.86).

Since $\sigma_{ij} = s_{ij} + \frac{1}{3}\delta_{ij}\sigma_{kk}$, it follows with evident notation that

$$\begin{aligned}tr(\boldsymbol{\sigma}\boldsymbol{M}^{(\alpha)}) &= tr(\boldsymbol{s}\boldsymbol{M}^{(\alpha)}) + \tfrac{1}{3}\sigma_{kk} \\ tr(\boldsymbol{\sigma}^2\boldsymbol{M}^{(\alpha)}) &= tr(\boldsymbol{s}^2\boldsymbol{M}^{(\alpha)}) + \tfrac{2}{3}\sigma_{kk}tr(\boldsymbol{s}\boldsymbol{M}^{(\alpha)}) + \tfrac{1}{9}\sigma_{kk}\sigma_{ss}\end{aligned} \tag{8.108}$$

Moreover, define the invariants

$$\boxed{\begin{array}{lll} I_{d1}=tr(s\boldsymbol{M}^{(1)}); & I_{d2}=tr(s\boldsymbol{M}^{(2)}); & I_{d3}=tr(s\boldsymbol{M}^{(3)}) \\ I_{d4}=tr(s^2\boldsymbol{M}^{(1)}); & I_{d5}=tr(s^2\boldsymbol{M}^{(2)}); & I_{d6}=tr(s^2\boldsymbol{M}^{(3)}) \end{array}} \tag{8.109}$$

Use of (8.108) and (8.109) in (8.107) results in

$$\begin{aligned} &\alpha_1(I_{d1}-I_{d2})^2+\alpha_2(I_{d1}-I_{d3})^2+\alpha_3(I_{d2}-I_{d3})^2 \\ &+\alpha_4(I_{d4}-I_{d1}^2)+\alpha_5(I_{d5}-I_{d2}^2)+\alpha_6(I_{d6}-I_{d3}^2) \\ &+\beta_1 I_{d1}I_{d2}+\beta_2 I_{d1}I_{d3}+\beta_3 I_{d2}I_{d3} \\ &+\frac{1}{9}\sigma_{kk}\sigma_{ss}(\beta_1+\beta_2+\beta_3) \\ &+\frac{1}{3}\sigma_{kk}\beta_1(I_{d1}+I_{d2})+\frac{1}{3}\sigma_{kk}\beta_2(I_{d1}+I_{d3}) \\ &+\frac{1}{3}\sigma_{kk}\beta_3(I_{d2}+I_{d3})-1=0 \end{aligned} \tag{8.110}$$

We want a criterion which is independent of the hydrostatic stress σ_{kk}. Thus, the parameters β_1, β_2 and β_3 are chosen such that the last four terms in front of the term -1 which involve the hydrastatic stress σ_{kk} disappear. Therefore

$$\beta_1=\beta_2=\beta_3=0 \tag{8.111}$$

Redefine the $\alpha_1\cdots\alpha_6$ parameters according to

$$\begin{array}{lll} \alpha_1=F; & \alpha_2=G; & \alpha_3=H \\ \alpha_4=L+M-N; & \alpha_5=N-M+L; & \alpha_6=N+M-L \end{array} \tag{8.112}$$

Finally, inserting (8.111) and (8.112) into (8.110) gives the result sought

Hill's criterion expressed in terms of structural tensors

$$\begin{aligned} &F(I_{d1}-I_{d2})^2+G(I_{d1}-I_{d3})^2+H(I_{d2}-I_{d3})^2 \\ &+(L+M-N)(I_{d4}-I_{d1}^2)+(N-M+L)(I_{d5}-I_{d2}^2) \\ &+(N+M-L)(I_{d6}-I_{d3}^2)-1=0 \end{aligned}$$

which corresponds to the result of Dafalias and Rashid (1989). Suppose that the coordinate axes are taken collinearly with the material directions; in that case the structural tensors are given by (8.104) and the expression above then reduces to the classical formulation given by (8.95).